



저작자표시 2.0 대한민국

이용자는 아래의 조건을 따르는 경우에 한하여 자유롭게

- 이 저작물을 복제, 배포, 전송, 전시, 공연 및 방송할 수 있습니다.
- 이차적 저작물을 작성할 수 있습니다.
- 이 저작물을 영리 목적으로 이용할 수 있습니다.

다음과 같은 조건을 따라야 합니다:



저작자표시. 귀하는 원저작자를 표시하여야 합니다.

- 귀하는, 이 저작물의 재이용이나 배포의 경우, 이 저작물에 적용된 이용허락조건을 명확하게 나타내어야 합니다.
- 저작권자로부터 별도의 허가를 받으면 이러한 조건들은 적용되지 않습니다.

저작권법에 따른 이용자의 권리는 위의 내용에 의하여 영향을 받지 않습니다.

이것은 [이용허락규약\(Legal Code\)](#)을 이해하기 쉽게 요약한 것입니다.

[Disclaimer](#) 

**Discovery of predictive marker genes for
the sensitivity for Gemcitabine plus
Abraxane (nab-paclitaxel) combination drug
in pancreatic cancer cell lines
using 3D organoid culture method**

Jin Su Kim

**The Graduate School
Yonsei University
Department of Medicine**

**Discovery of predictive marker genes for
the sensitivity for Gemcitabine plus
Abraxane (nab-paclitaxel) combination drug
in pancreatic cancer cell lines
using 3D organoid culture method**

**A Master's Thesis Submitted
to the Department of Medicine
and the Graduate School of Yonsei University
in partial fulfillment of the
requirements for the degree of
Master's of Medical Science**

Jin Su Kim

June 2024

**This certifies that the Master's Thesis
of Jin Su Kim is approved.**

Thesis Supervisor _____
Seungmin Bang

Thesis Committee Member _____
Galam Leem

Thesis Committee Member _____
Ho Kyoung Hwang

**The Graduate School
Yonsei University
June 2024**

ACKNOWLEDGEMENTS

I want to take this opportunity to express my heartfelt gratitude to the many individuals who supported, encouraged, and assisted me in my research as I conclude my master's degree program.

First and foremost, I am deeply grateful to Professor Seungmin Bang, my supervisor, for providing invaluable advice and guidance. His direction ensured that I stayed on course and successfully completed my study. I also extend my thanks to Professor Galam Leem and Professor Ho Kyoung Hwang for their insightful feedback, which helped me identify shortcomings, areas needing revision, and aspects I may have overlooked during my degree.

I want to express my gratitude to the research associate professor at our laboratory, Ph.D. Chan Hee Park, as well as researchers Jinyoung Lee, Eun Hee Kam, Yun Ji Kim, and Clinical Research Coordinators (CRC) Da Hei Yoon and Somin Shin for their tremendous help, support, and encouragement as I began my master's degree research, determined the direction and topic, and conducted experiments.

First, I extend my deepest thanks to Ph.D. Chan Hee Park, who provided the most help and advice from the beginning to the end of my degree and supported me in every way possible as if it were his own work. I am grateful to researcher Jinyoung Lee for her significant assistance in establishing the crucial cell lines for organoid research. I also thank researcher Eun Hee Kam for helping to solve various problems encountered during experiments and researcher Yun Ji Kim for her great help in preparing presentations and reviewing papers. Lastly, I would like to take this opportunity to thank CRC Da Hei Yoon and Somin Shin for their warm encouragement and support during challenging times.

I also extend my thanks to Professor Hee Seung Lee for his significant help and guidance in establishing the direction of research on the culture model set up for patient-derived pancreatic cancer cell line organoids, marking a pivotal achievement in pancreatic cancer organoid research. I also appreciate the support and encouragement from Professors Jeong Youp Park and Jung Hyun Jo throughout my master's degree research. Furthermore, I am grateful to M.D. Ji Hoon Kim, M.D. Won Joon Jang, M.D. Kyung In Shin, M.D. Ji Young Keum, researcher Yoo Keung Tae, and CRC Soo Jeong Jang for their encouragement and support.

To my beloved father, mother, brother, sister-in-law, and lovely nephew, your unwavering support and prayers have meant more to me than words can express. Lastly, I want to extend my sincere thanks to my dear relatives, supportive friends, pastor, and secretaries of the church for their warm encouragement and unwavering backing. Finally, I want to thank God for guiding me and helping me stay on the right path from the beginning to the end.

TABLE OF CONTENTS

LIST OF FIGURES	iii
LIST OF TABLES	iv
ABSTRACT IN ENGLISH	v
1. INTRODUCTION	1
2. MATERIALS AND METHODS	3
2.1. Cell lines and cell culture conditions	3
2.2. Matrigel-based 3D organoid culture	3
2.3. Paraffin embedding (PE) organoid block	3
2.4. Immunofluorescence (IF) analysis	4
2.5. Organoid tissue microarray (OTMA)	4
2.6. Cell viability and drug sensitivity	5
2.7. Omics analysis – RNA sequencing	5
2.8. Quantitative real-time reverse transcription polymerase chain reaction (qRT-PCR)	6
2.9. Western blotting	7
2.10. Immunohistochemistry (IHC) analysis	7
2.11. Statistical analysis	8
3. Results	9
3.1. Research flow chart using established pancreatic cancer organoids	9
3.2. Matrigel-based 3D organoid culture model set up using pancreatic cancer cell lines	11
3.3. Established CRC YPAC cell line organoids characterization	13
3.4. Design and manufacture of organoid tissue microarray (OTMA)	15
3.5. Set up of matrigel-based 3D organoid drug test platform for pancreatic cancer cell lines	17
3.6. Screening of GA combination drug sensitivity using established pancreatic cancer cell line organoids	19
3.7. Pancreatic cancer cell line organoids transcriptome analysis (RNA-Seq)	21
3.8. GA combination drug predictive marker genes selection	23
3.9. Confirmation of predictive marker genes mRNA expression using established pancreatic cancer cell line organoids	25
3.10. Confirmation of predictive marker genes protein expression using established pancreatic cancer cell line organoids	28

3.11 Validation of predictive marker genes using established CRC YPAC cell line organoids	31
4. DISCUSSION	34
5. CONCLUSION	38
REFERENCES	39
ABSTRACT IN KOREAN	49

LIST OF FIGURES

<Figure 1> Research flow chart	10
<Figure 2> Establishment of matrigel-based 3D organoid culture model using pancreatic cancer cell lines	12
<Figure 3> Characterization of established CRC YPAC cell line organoids	14
<Figure 4> Design and prepare the organoid tissue microarray (OTMA)	16
<Figure 5> Optimization of drug sensitivity using established pancreatic cancer cell line organoids	18
<Figure 6> Pancreatic cancer cell line organoids GA combination drug sensitivity	20
<Figure 7> Transcriptome analysis	22
<Figure 8> Predictive marker genes selection	24
<Figure 9> Correlation of mRNA expression between RNAseq and qRT-PCR	26
<Figure 10> Confirmation of GA combination drug predictive marker genes protein expression	29
<Figure 11> IL4R and S100A4 IHC and IC50 values of GA combination drug in established CRC YPAC cell line organoids	32

LIST OF TABLES

<Table 1> PCR primer sequences and conditions.....	27
<Table 2> Comparison of GA combination drug predictive marker genes IHC H-score in established pancreatic cancer cell line organoids.....	30
<Table 3> Comparison of GA combination drug predictive marker genes IHC H-score in established CRC YPAC cell line organoids.....	33

ABSTRACT

Discovery of predictive marker genes for the sensitivity for Gemcitabine plus Abraxane (nab-paclitaxel) combination drug in pancreatic cancer cell lines using 3D organoid culture method

Pancreatic cancer remains a lethal malignant disease with a 5-year survival rate of less than 10%. More than 80% of pancreatic cancer patients are diagnosed at a stage where surgical resection is not an option, necessitating chemotherapy. However, since there is no biomarker for patient-specific drug selection yet, it is essential to discover biomarkers for pancreatic cancer patients.

One of the first attempts in this direction was the establishment of adherent pancreatic cancer cell lines (2D) from patients' tumors. For decades, these 2D pancreatic cancer cell lines have been used as convenient PDAC models. However, 2D cells differ somewhat from the characteristics of early tumors in several aspects, including tumor microenvironment, metabolism, sensitivity to anticancer drugs, and gene expression. To reduce these differences, 3D tumor organoid culture methods have recently been developed for various cancer types affecting organs such as the pancreas, prostate, liver, stomach, and lung. Organoids are capable of reproducing the morphology, gene and protein expression, cell polarity, and cellular metabolic heterogeneity of the primary tumor to a large extent. As a result, they serve as an ideal tool for modeling pancreatic cancer and conducting drug testing.

In this study, to enhance the therapeutic effect of pancreatic cancer by identifying predictive marker genes for the efficacy of the gemcitabine plus Abraxane (nab-paclitaxel) combination drug, we established a matrigel-based 3D organoid culture model and organoid drug test platform using pancreatic cancer cell lines in normal cell culture media condition and patient-derived pancreatic cancer cell lines (CRC YPAC cell lines) in F-media condition, without using organoid culture media. Subsequently, utilizing the established organoid culture model and drug test platform, we identified IL4R as a sensitivity biomarker and S100A4 as a resistance biomarker for the gemcitabine plus Abraxane (nab-paclitaxel) combination drug in pancreatic cancer.

Key words : pancreatic cancer cell lines, gemcitabine plus abraxane (nab-paclitaxel) combination drug, 3d organoid culture model, predictive marker genes

1. INTRODUCTION

Pancreatic cancer is a fatal tumor in humans, it is expected to represent the second leading cause of cancer-related death in western countries by 2040.^{1,2} During the last three decades, treatment outcome of pancreatic cancer was not significantly improved with only 10% of 5-year survival.¹ This is attributed to hardness of early diagnosis and relatively high risk of recurrence even after curative resection of pancreatic cancer.³⁻⁵

For decades, conventional cell culture models (2D culture) have served as convenient models for studying PDAC, offering significant advantages in terms of ease of handling for researchers, continuous culture capability, and reasonable cost.⁶ However, 2D cells have been found to significantly diverge from the original tumor in various aspects, including the tumor microenvironment, cell metabolism, and gene expression.⁷⁻⁹ To address the limitations of 2D culture models, recently developed 3D cell culture technologies have led to the creation of novel and more physiologically accurate models for human healthy tissue and cancer.¹⁰ Furthermore, several studies have reported differences in biological phenotypes, molecular mechanisms, and drug responses between 2D and 3D culture models.^{11,12} The establishment of 3D culture models remains highly significant for PDAC-related research.

The realm of 3D cell culture technologies encompasses two main methods with extracellular matrix space, such as scaffold-free models, and scaffold-based models. The scaffold-free method employs an anti-adhesion approach, involving either coating the bottom with cell adhesion paper or continuously flowing culture fluid to prevent cell adhesion (Spheroid culture).¹³⁻¹⁶ In the scaffold-based method, an artificial polymer, such as a solid scaffold or hydrogel, serves as an extracellular matrix.¹⁷⁻²⁵ In scaffold-based models, the organoid culture model is undoubtedly a highly discussed topic. This culture protocol has served as the foundation for various other organoid culture protocols involving multiple mouse and human organs, including the pancreas, prostate, liver, stomach, and lung.^{21,26-30} Organoids thrive within a basement membrane extract (BME), such as an extracellular matrix (ECM)-based hydrogel (Matrigel), which allows them to grow in a 3D structure reminiscent of organs while preserving heterogeneity in terms of cellular and molecular composition *ex vivo*. Organoids have the potential to build biobanks, making them immensely valuable in advancing new drug development for precision and personalized medicine.^{26,27} Additionally, organoids closely

replicate the morphology, gene and protein expression, cell polarity, and cellular metabolic heterogeneity of primary tumors to a significant extent. This characteristic renders them an exceptional tool for modeling PDAC and conducting drug testing.^{31,32}

The currently preferred regimens, such as FOLFIRINOX (5-fluorouracil, folinic acid, irinotecan, oxaliplatin), or GA (gemcitabine plus nab-paclitaxel (Abraxane)), do not extend patient survival by more than 12 months.³⁻⁵ Despite efforts to address this, various biomarkers and new target treatments have been studied for patient-specific drug selection. However, thus far, no biomarkers or target treatments have demonstrated success.^{33,34}

In this study, to enhance the therapeutic effect of the GA combination drug for pancreatic cancer patients, we aim to identify marker genes for predicting the efficacy of the GA combination drug using the matrigel-based 3D organoid culture method and drug test platform in normal cell culture media and F-media culture conditions, not using organoid culture media.

2. MATERIALS AND METHODS

2.1. Cell lines and cell culture conditions

The following human pancreatic cancer cell lines were used: AsPC-1, Capan-1, Capan-2, MIA PaCa-2, PANC-1 cells were purchased from the Korea Cell Line Bank (KCLB, Republic of Korea) and BxPC-3, CFPAC-1, HPAC cells were purchased from the American Type Culture Collection (ATCC, Manassas, VA, USA). Patient-derived pancreatic cancer cell lines were used in our laboratory to establish CRC YPAC cell lines.^{35,36} PANC-1, MIA PaCa-2 cells were cultured in DMEM/HIGH (HyClone, catalog no. SH30243.01, USA) with 10% FBS (Thermo Scientific, catalog no. 12483020, USA). AsPC-1, BxPC-3, Capan-1, Capan-2, CFPAC-1 cells were cultured in RPMI1640 (HyClone, catalog no. SH30027.01, USA) with 10% FBS (Thermo Scientific, catalog no. 12483020, USA). CRC YPAC cells were cultured in F-media consisted of 70% Ham's F-12 nutrient mix (HyClone, catalog no. SH30026.01, USA) and 25% in DMEM/HIGH (HyClone, catalog no. SH30243.01, USA) with 5% FBS (Thermo Scientific, catalog no. 12483020, USA) and Rho-kinase inhibitor (Y-27632) (Sigma-Aldrich, catalog no. Y0503, USA) as previously reported in our laboratory conditionally reprogrammed cell culture method.^{35,36} All pancreatic cancer cell lines were cultured at a 37°C in incubator with 5% CO₂.

2.2. Matrigel-based 3D organoid culture

Before cell seeding, mix the cells with 90% Growth Factor Reduced Matrigel (Corning, catalog no. 356231, USA). After then, the cells will be seeded in a 6-well plate (SPL, catalog no. 30006, Republic of Korea) at a density of 5,000 to 10,000 cells per 20 µl of matrigel/cell mixture generated per well of the 6-well plate (7 drops per well). Allow the resulting cell suspension to solidify on the 6-well cell culture plate at 37°C for 20 minutes. After 20 minutes, add 4 mL of culture media to the 6-well cell culture plate. The culture medium should be refreshed every 3-4 days.^{37,38}

2.3. Paraffin embedding (PE) organoid block

To paraffin-embed the organoids, after 2-4 weeks when the organoids reached a size of 200-

300 μ m, they were fixed in 4% paraformaldehyde (PFA) at 4°C for 60 minutes. Then the fixed organoids dissociated from the matrigel, washed with PBS and suspended in 3% ultra-low gelling temperature (ULGT) agarose (Sigma-Aldrich, catalog no. A2576, USA), then incubated at 4°C for 10 to 15 minutes for gelation. Each of the solidified ULGT agarose organoid buttons is transferred into the cap of the 5ml snap tube (SPL, catalog no. 50005, Republic of Korea). Then, using the cap as a mold, place the solidified ULGT agarose organoid buttons at the bottom and filled the cap with 1% agarose (Sigma-Aldrich, catalog no. A9918, USA). Remove the solidified agarose gel disk for the cap and then subjected to tissue processing for paraffin embedding with manufacture's protocol.³⁹⁻⁴³

2.4. Immunofluorescence (IF) analysis

Immunofluorescence (IF) was performed on OTMA slide. IF staining was conducted after antigen retrieval, which involved boiling slides in 10mM sodium citrate buffered distilled water (pH 6.0) for 30 minutes in a 97°C water bath, followed by a 30-minute cool down period. Each organoid slide was incubated with the first primary antibodies, cytokeratin (Santa Cruz Biotechnology, catalog no. sc-6278, 1:100, USA) and vimentin (Cell Signaling, catalog no. D21H3, dilution 1:100, USA), overnight at 4°C. After washing three times, the slides were incubated with secondary antibodies, Alexa Fluor 594 (Invitrogen, catalog no. A-11012, dilution 1:400, USA) and Alexa Fluor 488 (Invitrogen, catalog no. A-11001, dilution 1:400, USA), for 1 hour at room temperature. Following another three washes, the slides were mounted using a mounting solution containing DAPI (Vector Laboratories, catalog no. H-1200, USA). Immunofluorescence images were acquired using Olympus BF53 microscopy (Olympus Life Science, Japan).

2.5. Organoid tissue microarray (OTMA)

For the organoid microarray (OMA), we used a total of 40 organoid PE blocks (8 pancreatic cancer cell lines and 32 YPAC CRC cells). We designed an organoid tissue microarray (OTMA) map with 3.0 mm diameter 40 core (8 by 5 grids) and recorded the core locations. Following the OTMA map, each PE block punched 3mm recipient needle in the recipient block at the target location. Afterwards, we gently and slowly poured melted paraffin into the drilled recipient block to allow the organoid

cores to adhere to the recipient block. We then incubated the OTMA block at 60°C for 20 minutes in an oven and stored at room temperature. The production of the OTMA block was conducted at the Biomedical Research Center at Gangnam Severance Hospital, Yonsei University

2.6. Cell viability and drug sensitivity

The cell viability assay performed to determine the drug sensitivity of each pancreatic cancer cell line organoids and CRC YPAC cell line organoids. Before cell seeding, mix the cells with 90% matrigel. Then, the cells were seeded in 48-well plates (SPL, catalog no. 30048, Republic of Korea) at a density of 5,000 cells per well. To identify compounds that are toxic to pancreatic cell line organoids and CRC YPAC cell line organoids, after 4 days, the organoids were exposed to different concentrations (0.01, 0.1, 1, 10, 100 X doses and 1X dose; gemcitabine 1 uM plus Abraxane 0.125 uM) of Gemcitabine plus Abraxane (nab-paclitaxel) combination drug for 3 days. Cell viability was measured by assessing cell viability after 3 days of treatment using CellTiter-Glo 3D reagent (Promega, catalog no. G9638, USA), according to the manufacturer's instructions. The assay was performed in triplicate.⁴⁴⁻⁴⁸ The data plots of cell toxicity extraction and proliferation will be generated using SigmaPlot software (Grafiti LLC, version 10.0, USA) and inhibitory concentration (IC50) values will be calculated using the CompuSyn software (ComboSyn Inc, version 1.0, USA).

2.7. Omics analysis – RNA sequencing

Total RNA was extracted from each sample using RNeasy Lipid Tissue Kit (Qiagen, Germany) with the manufacturer's instructions and quantity and quality of extracted total RNA were measured by NanoDrop 8000 Spectrophotometer (Thermo Scientific, USA) and Agilent 2100 Bioanalyzer, respectively (Agilent Technologies, USA). For the sequencing, ~ 2.5ug of total RNA was prepared for cDNA library synthesis according to the Illumina TrueSeq RNA Sample Preparation Kit (Illumina, catalog no. RS-122-2001, USA) protocol. The synthesized library was then amplified, and the final library yielded ~400 ng of cDNA. The resulting cDNA libraries (for all four samples) were then paired-end sequenced (2 × 150 bp) with NextSeq (Illumina HiSeq 2000/1000 and HiScanSQ, USA). The preprocessing was performed using galaxy project (<https://usegalaxy.org>). We trimmed the FASTQ files to obtained clean cropped read with length 100 using trimmomatic

from the paired-end sequence files. RNA STAR and Feature count are mapped the read to transcriptome as a reference and calculated normalized gene-level expression values such as Fragments Per Kilobase Million (FPKM). For the selection of differentially expressed genes (DEGs) were selected based on more than a 2-fold difference between the GA combination drug-sensitive and -resistant groups, with a p-value of less than 0.05, using the Microsoft Excel program (Excel 2016, USA). Hierarchical clustering and correlation matrix analysis were performed using a complete linkage algorithm with pearson correlation using the Idep.96 bioinformatics software (<http://bioinformatics.sdstate.edu/idep96/>). The principal component analysis (PCA) visualizations were generated and visualized using the ExpressAnalyst software (<https://www.expressanalyst.ca/ExpressAnalyst/home.xhtml>).

2.8. Quantitative real-time reverse transcription polymerase chain reaction (qRT-PCR)

Total RNA was extracted from pancreatic cancer cell line organoids using the AllPrep DNA/RNA/miRNA Universal Kit (QIAGEN, catalog no. 80024, Germany). Complementary DNA (cDNA) synthesis was performed using the AccuPower CycleScript RT PreMix (dN6) kit (BIONEER, catalog no. K-2046, Republic of Korea). The PCR primers were based on the sequence of each gene from National Center for Biotechnology (NCBI, <https://www.ncbi.nlm.nih.gov/>) information, and primer sequences were summarized in Table 1. PCR was performed using the Takara Taq PCR Kit (TAKARA, catalog no. R001A, Japan). All reactions were run in PCR STRIP TUBES (AXYGEN, catalog no. PCR-0208-CP-C, USA) with a total volume of 25 μ l. One negative control and samples were included in each run. All steps were carried out according to the manufacturer's protocols. The PCR programs for each run were summarized in Table 1. After the reaction, the samples were loaded on a 2% agarose gel with 6X loading dye (DYNEBIO, catalog no. A750, Republic of Korea) and analyzed by gel electrophoresis using a Gel Documentation System (Carestream, Model 210 pro, USA). Quantitative RT-PCR was performed using Power SYBR Green PCR Master Mix (Thermo Fisher, catalog no. 4367659, USA). In this experiment, all reactions were in MicroAmp Fast 96-Well Reaction Plate 0.1ml (Applied Biosystems, catalog no. 4346907, USA) with a total volume of 20 μ l. The reaction mixture consisted of 7 μ l DDW, 10 μ l of 2X SYBR Green PCR Master Mix, 1 μ l of cDNA, and 0.5pmol of forward and reverse primers in each experiment.

Each experiment using quantitative RT-PCR (Applied Biosystems, Model Quantstudio 3, USA) was performed in triplicate. The expression of predictive marker genes mRNA was quantified relative to GAPDH expression.

2.9. Western blotting

Protein extracts were obtained from pancreatic cancer cell line organoids using a RIPA buffer (Thermo Fisher, catalog no. 89901, USA) containing protease and phosphatase inhibitors (Thermo Fisher, catalog no. 78442, USA). Equal amounts of protein will be loaded in each lane of an SDS-10-12% polyacrylamide gel. Primary antibodies used for western blot analysis LPCAT1 (Proteintech, catalog no. 161121-1-AP, dilution 1:500, USA), ITGA6 (Proteintech, catalog no. 27189-1-AP, dilution 1:500, USA), IL4R (Proteintech, catalog no. 28331-1-AP, dilution 1:500, USA), S100A4 (Abcam, catalog no. ab197896, dilution 1:5000, USA) and GAPDH (Santa Cruz Biotechnology, catalog no. sc-47724, dilution 1:1000, USA). The protein levels were quantified using ImageJ analysis software (NIH, version 1.8.0, USA).

2.10. Immunohistochemistry (IHC) analysis

Immunohistochemistry (IHC) was performed on OTMA slide. IHC staining was conducted after antigen retrieval by boiling slides in 10mM sodium citrate buffered distilled water (pH 6.0) for 30 minutes in a 97°C water bath, followed by a 30-minute cool down period. Each organoid slides were incubated in first primary antibody, LPCAT1 (Proteintech, catalog no. 161121-1-AP, dilution 1:500, USA), IL4R (Proteintech, catalog no. 28331-1-AP, dilution 1:1000, USA) and S100A4 (Abcam, catalog no. ab197896, dilution 1:5000, USA) overnight at 4°C. The Dako REAL Peroxidase Detection System Kit (Dako, catalog no. K5007, USA) was used as per the manufacturers' specifications, which included the use of the ready-to-use anti-rabbit/mouse secondary antibody. Finally, the sections were counterstained with hematoxylin solution (Sigma-Aldrich, catalog no. 03971, USA). After three times washing, the slides were mounted using permount mounting medium (Fisher chemical, catalog no. SP15-100, USA). The immunohistochemical images were acquired using Zeiss Axioscan 7 digital whole slide scanner (Zeiss, Germany) and the IHC histoscore (H-score) was calculated as 0 (negative), 1 (low positive),

2 (positive), and 3 (high positive) by the proportion of positive cells from the OTMA IHC staining images.

2.11. Statistical analysis

All statistical analyses were performed using Microsoft Excel (Excel 2016, USA). A regression analysis was conducted between the marker gene IHC positive area (X-axis) and GA combination drug IC50 (Y-axis). IC50 values were statistically analyzed using Student's t-test. The established CRC YPAC organoids were divided into two groups: sensitive (GA combination drug IC50 < Median) and resistant (GA combination drug IC50 > Median). They were further divided based on the IL4R/S100A4 H-score ratio into high (H-score ratio > Median) and low (H-score ratio < Median). Overall survival (OS) according to IL4R and S100A4 was estimated and visualized using the Kaplan-Meier method (<http://dosurvive.lab.nycu.edu.tw/>). Differences between groups were considered significant at a p-value of < 0.05.

3. RESULTS

3.1. Research flow chart using established pancreatic cancer organoids

To establish the 3D matrigel-based organoid culture model, first we used a pancreatic cancer cell line and successfully established both pancreatic cancer cell line and CRC YPAC cell line organoids both. The established organoids showed different morphologies and maintained the characteristics of their origins. Next, utilizing the established pancreatic cancer cell line and CRC YPAC cell line organoids, we created an organoid biobank, paraffin-embedded (PE) organoid blocks, and a drug test platform. Finally, using these organoid samples and the drug test platform, we performed RNA-seq, qRT-PCR, and western blot analyses to discover and validate GA combination drug predictive marker genes.

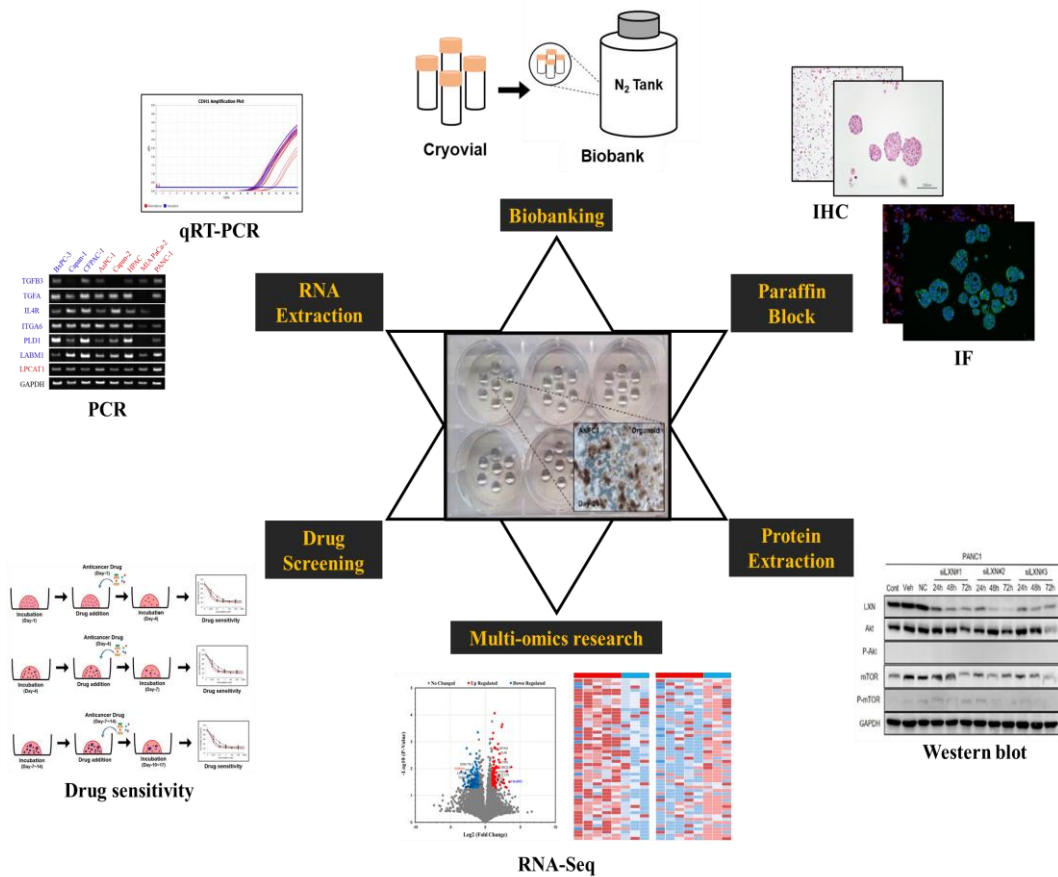


Figure 1. Research flow chart. Using a matrigel-based 3D organoid culture model, we established 8 pancreatic cancer cell lines and CRC YPAC cell line organoids more than 40 cells. Subsequently, we utilized the established organoids to perform immunohistochemistry (IHC) and immunofluorescence (IF), drug screening, RNA-seq, RT-PCR, qRT-PCR, and western blot.

3.2. Matrigel-based 3D organoid culture model set up using pancreatic cancer cell lines

To establish a suitable matrigel-based 3D organoid culture model for pancreatic cancer cell lines, we used AsPC-1 and PANC-1 cell lines for organoid culture model set up. First, we selected a 6-well cell culture plate for 3D organoid culture within each well of 6-well cell culture plate, a density of 5,000 to 10,000 cells per matrigel plus cell mixture (20 μ l) was seeded and cultured in normal cell culture media condition, not using organoid culture media. AsPC-1 and PANC-1 organoids observed under bright-field microscopy, typically appeared within 1 week after cell seeding, and after 3 weeks, the cultures were stopped when the diameter of the organoids reached up to 200-300 μ m and established organoids showed different morphologies (Figure 1A). One of the most significant advantages of organoids is their ability to reflect the unique characteristics of cells.^{31,32} Based on previous research, we confirmed that the matrigel-based 3D organoid culture model maintained the unique characteristics of the cells. We performed immunofluorescence staining using the ductal epithelial marker cytokeratin 19 (CK-19), the fibroblast marker vimentin, and islet cell marker insulin and acinar cell marker α -amylase.^{35,36} Immunofluorescence staining results showed that the insulin and α -amylase were not stained, while the CK-19 was strongly stained in both AsPC-1 and PANC-1 organoids. The vimentin was only strongly stained in the PANC-1 organoid. (Figure 2B). Specifically, in pancreatic cancer cell lines, two types of cells mainly express epithelial or mesenchymal molecules, PANC-1 has been classified as mesenchymal cells, and AsPC-1 has been classified as epithelial cells.⁴⁹ Subsequently, we established eight pancreatic cancer cell line organoids, each showing different morphologies. AsPC-1 and BxPC-3 organoids showed compact-like morphology, while Capan-1, Capan-2, CFPAC-1, and HPAC organoids showed tubular-like morphology. MIA PaCa-2 and PANC1 organoids showed scattered-like morphology under BFM and H&E images (Figure 2C).

Through these results, we successfully established a matrigel-based 3D organoid culture model using pancreatic cancer cell lines in normal cell culture media condition, not using organoid culture media and the established organoids exhibited different morphologies. Furthermore, we demonstrated that the matrigel-based 3D organoid culture model can reflect the epithelial and mesenchymal characteristics of each pancreatic cancer cell type.

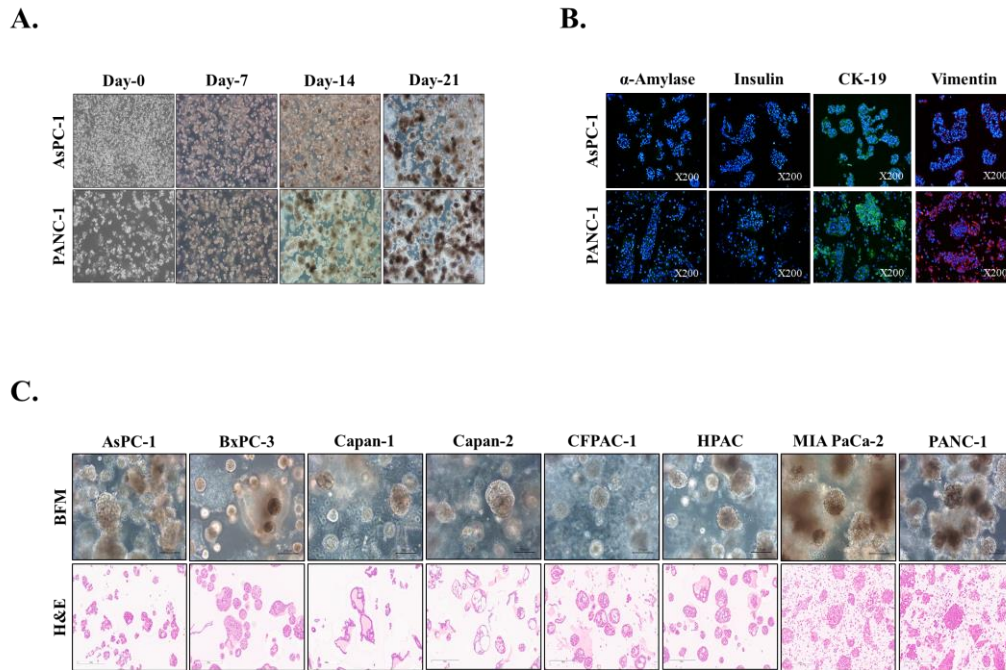


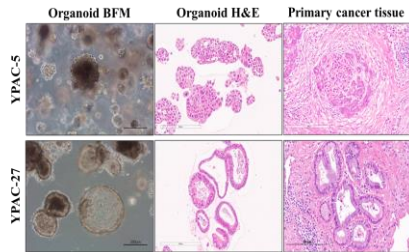
Figure 2. Establishment of matrigel-based 3D organoid culture model using pancreatic cancer cell lines. (A) Serial images of growing pancreatic cancer cell line organoids (Day-0, 7, 14, 21), scale bar: 200 μ m. (B) Ductal epithelial marker CK-19, fibroblast marker vimentin, islet cell marker insulin and acinar cell marker α -amylase immunofluorescence (IF) staining images of AsPC-1 and PANC-1 organoids, scale bar: 50 μ m (C). BFM and H&E matching images of established pancreatic cancer cell line organoids, scale bar:200 μ m. Blue, DAPI; Green, a-amylase, insulin and CK-19; Red, vimentin, CK-19; cytokeratin, BFM; bright field microscope, H&E; hematoxylin and eosin.

3.3. Established CRC YPAC cell line organoids characterization

In previous results, using the matrigel-based 3D organoid culture model, we successfully established pancreatic cancer cell line organoids in normal cell culture media conditions, not using organoid culture media and demonstrated that this model can reflect the characteristics of each cell type. To further utilize this matrigel-based 3D organoid culture model, we try to established of patient-derived pancreatic cancer organoids using patient-derived conditionally reprogrammed cell lines (CRC YPAC cell lines) in our laboratory using F-media culture condition, not using organoid culture media. First, among the established CRC YPAC cell lines, organoid culture was performed using YPAC-5 and YPAC-27 with primary cancer tissues. The formed YPAC-5 organoid showed a compact-like morphology, while the YPAC-27 organoid exhibited a tubular-like morphology. It was confirmed that these morphologies were very similar to the primary cancer tissues (Figure 3A). Immunofluorescence staining results showed that insulin, α -amylase, and vimentin were not stained, but CK-19 was clearly stained (Figure 3B). CRC YPAC organoid immunofluorescence staining results matched the CRC YPAC 2D immunofluorescence staining results from previously published research in our laboratory.³⁶

Through these results, we successfully established the CRC YPAC cell line organoids in F-media culture condition, not using organoid culture media. Additionally, the matrigel-based 3D organoid culture model replicated the morphological features of primary cancer tissues and revealed the unique characteristics of their origin.

A.



B.

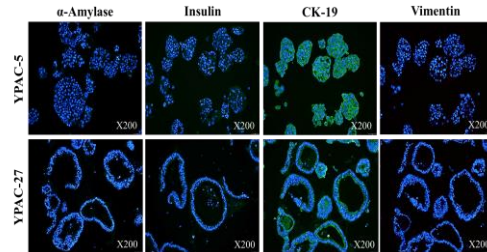


Figure 3. Characterization of established CRC YPAC cell line organoids. (A) Matching images of CRC YPAC cell line organoids and primary cancer tissues show that the established CRC YPAC cell line organoids have morphological and histological similarities to primary cancer tissue, scale bar: 200 μm . (B). IF staining images of established CRC YPAC cell line organoids confirm the preservation of 2D marker expression patterns in the organoids, scale bar: 50 μm Blue, DAPI; Green, α -amylase, insulin and CK-19; Red, vimentin, CK-19; cytokeratin; BFM, bright field microscope; H&E, hematoxylin and eosin.

3.4. Design and manufacture of organoid tissue microarray (OTMA)

To establish efficient organoid IHC methods, we were thinking of organoid tissue microarray (OTMA) construction. Specifically, TMA methods were considered a powerful and efficient tool for high-throughput screening (HTS).⁵⁰⁻⁵³ Considering time and cost, this method is very effective.^{50,52} First, we measured the diameter of the established PE organoid block core to determine the suitable core size and count for OTMA construction. Considering the average diameter of the established PE organoid block core size, a 3.0 mm diameter with 40 cores is most suitable for the construction of OTMA. Next, using the established PE organoid blocks (40 cases), we constructed the OTMA block was completed. Constructed OTMA block A1 to A8 cores consisted of pancreatic cancer cell line organoids, while block B1 to E8 cores consisted of CRC YPAC cell line organoids. Finally, after comparing the H&E staining images of OTMA before constructing the OTMA block with the PE organoid H&E staining images, both sets of H&E staining images were found to be equivalent.



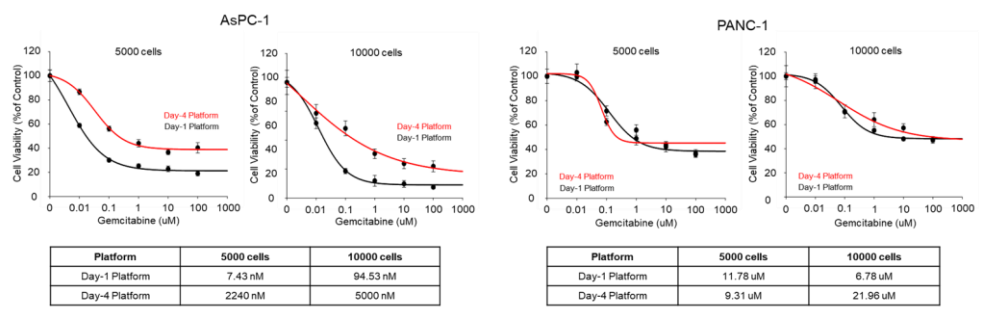
Figure 4. Design and prepare the organoid tissue microarray (OTMA). Construction of organoid tissue microarray (OTMA) using established 8 pancreatic cancer cell line PE organoid blocks and 32 CRC YPAC cell line PE organoid blocks (total 40 blocks). The constructed OTMA blocks consisted of 40 cores: A1 to A8 cores were pancreatic cancer cell line organoids, and the remaining 32 cores were CRC YPAC cell line organoids.

3.5. Set up of matrigel-based 3D organoid drug test platform for pancreatic cancer cell lines

In pancreatic cancer, previously reported that 3D culture is a better model for drug testing⁵⁴ and organoids have the potential to new drug development for precision and personalized medicine.²⁶ Based on a previous report, we designed several matrigel-based 3D organoid drug test platforms to establish a suitable platform for pancreatic cancer cell lines.

To evaluate and confirm the drug test platform, we utilized the AsPC-1 and PANC-1 cell lines and compared the cell numbers and incubation days for pancreatic cancer cell line organoids using gemcitabine (Figure 5A). Specifically, in repeated experiments, the 5000-cell day-4 drug test platform was found to be the most suitable for pancreatic cancer cell line organoids. Based on these testing results, we selected the 5000-cell day-4 drug test platform for pancreatic cancer cell line organoids (Figure 5B).

A.



B.

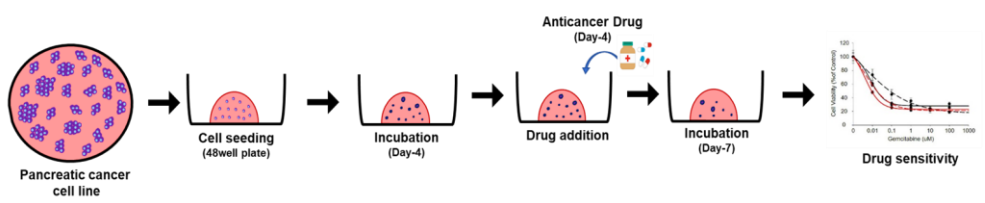
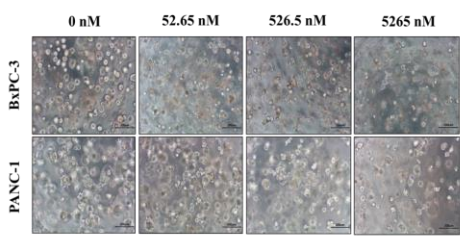


Figure 5. Optimization of drug sensitivity using established pancreatic cancer cell line organoids. (A) Matrigel-based 3D organoid drug test platforms comparison test using AsPC1 and PANC-1 organoids. (B) Establishment of 5000-cell day-4 drug test platform for pancreatic cancer cell line organoids.

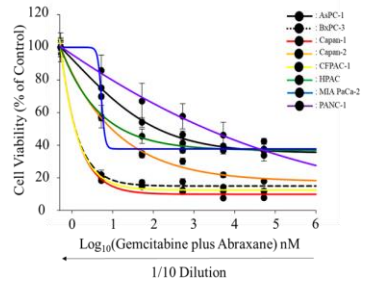
3.6. Screening of GA combination drug sensitivity using established pancreatic cancer cell line organoids

Next, we assessed the sensitivity of 8 pancreatic cancer cell line organoids to the GA combination drug using a 5000-cell, day-4 drug test platform. Established pancreatic cancer cell line organoids showed heterogeneity in their response to GA combination drug. In bright field microscopy images, the morphologies of the BxPC-3 and PANC-1 organoids were distinguishable at both low and high doses of the GA combination drug (Figure 6A). In GA combination drug sensitivity screening, BxPC-3, Capan-1, and CFPAC1-1 showed a sensitive response to the GA combination drug, while AsPC-1, Capan-2, HPAC, MIA PaCa-2, and PANC-1 did not (Figure 6B). Finally, based on GA IC50 results, we categorized the pancreatic cancer cell line organoids into two groups: the sensitive group, which includes CFPAC-1, BxPC-3, and Capan-1; and the resistance group, which includes AsPC-1, Capan-2, HPAC, MIA PaCa-2, and PANC-1 (Figure 6C).

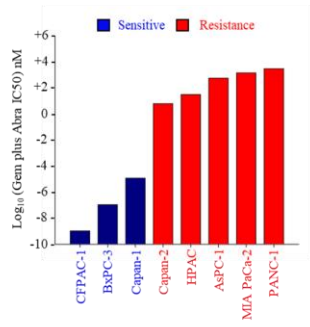
A.



B.



C.



Gemcitabine plus Abraxane drug sensitivity								
Cell lines	CFPAC-1	BxPC-3	Capan-1	Capan-2	HPAC	AsPC-1	MIA PaCa-2	PNAC-1
Log ₁₀ (GA IC ₅₀) nM	-8.98	-6.96	-4.93	0.80	1.51	2.76	3.16	3.48
GA Response	Sensitive	Sensitive	Sensitive	Resistance	Resistance	Resistance	Resistance	Resistance

Figure 6. Pancreatic cancer cell line organoids GA combination drug sensitivity. (A) Morphology changes of BxPC-3 and PANC-1 organoids in different GA combination drug concentration, scale bar: 200 μ m. (B) Pancreatic cancer cell line organoid GA combination drug sensitivity. (C) Categorized the pancreatic cancer cell line organoids into two groups: sensitive and resistance, based on their response to the GA combination drug.

3.7. Pancreatic cancer cell line organoids transcriptome analysis (RNA-Seq)

Through the analysis of sensitivity to the GA combination drug in pancreatic cancer cell line organoids, the cell line organoids were grouped based on their response sensitive or resistant to the GA combination drug. Based on RNAseq analysis of 8 pancreatic cancer cell line organoids, before analyzing the differences in expressed genes between the two groups, we first checked the gene expression patterns of 8 pancreatic cancer cell line organoids. The unsupervised genes hierarchical clustering heatmap showed that the drug-sensitive and resistant groups were not distinguishable (Figure 7A). In the principal component analysis (PCA), the drug-sensitive and resistant groups were not clustered into separate groups (Figure 7B). Secondly, to identify predictive marker genes for the GA combination drug, we compared the sensitive and resistant groups. Genes with expressions up or down regulated more than $\log_2(\text{fold change}) > 1$ and a $p\text{-value} < 0.05$ were selected for the list of differentially expressed genes (DEGs). Through this process, we identified 236 DEGs between the two groups. In the volcano plots, the 236 DEGs were well distributed (Figure 7C). Additionally, in the hierarchical clustering heatmap (Figure 7D). and PCA (Figure 7E), the 236 DEGs clustered well into their respective groups.

These results indicate that by narrowing down the unsupervised genes to 236 DEGs, we were able to confirm that the differences between the two groups could be clearly distinguished.

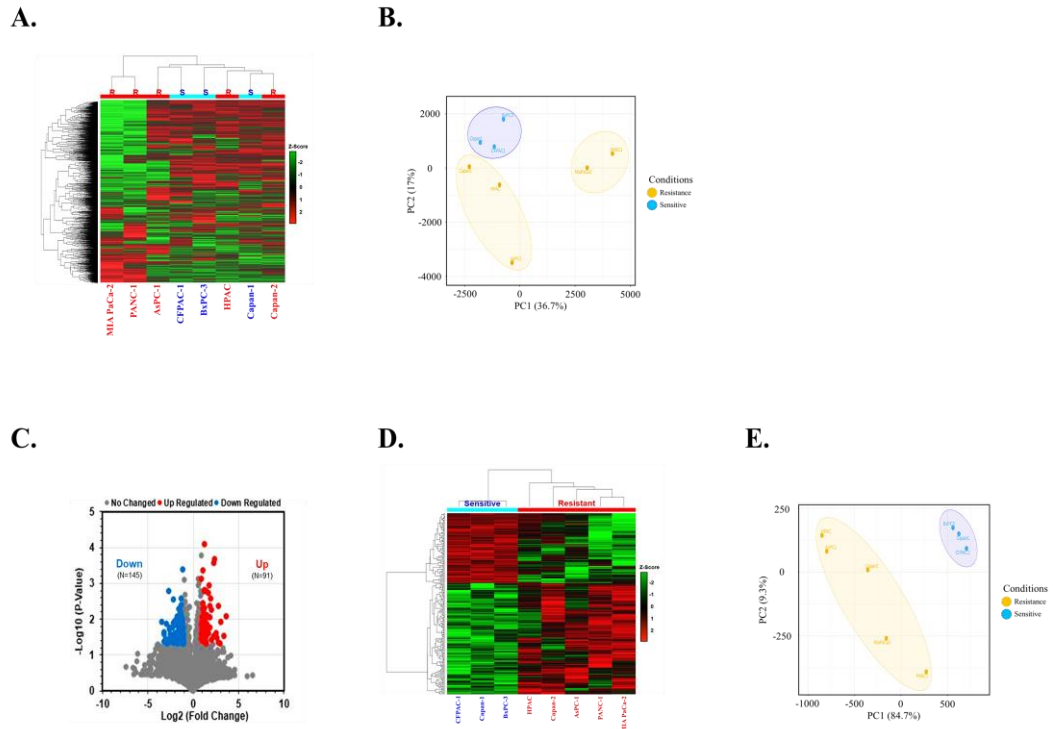
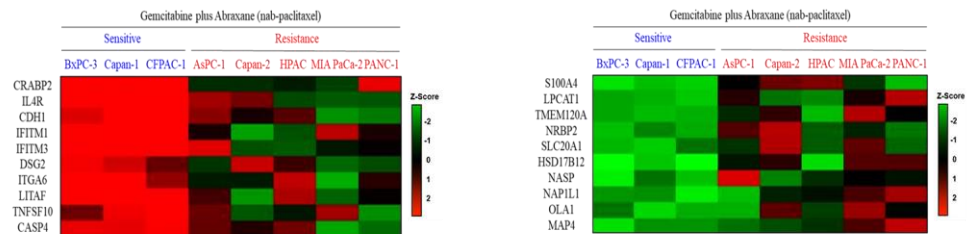


Figure 7. Transcriptome analysis. Unsupervised hierarchical clustering heatmap (A) and principal component analysis (PCA) (B) using whole transcriptome after RNAseq analysis. (C) DEGs volcano between GA combination drug resistance and sensitive groups. Heatmap of supervised hierarchical clustering (D) and PCA (E) using selected 236 DEGs. Red indicates upregulated genes, and blue indicates downregulated genes in the heatmap. Red scatters indicate upregulated genes, blue scatters indicate downregulated genes, and gray scatters indicate no DEGs in the volcano plot. Orange indicates the resistance group, and blue indicates the sensitive group in the PCA.

3.8. GA combination drug predictive marker genes selection

Based on the list of 236 DEGs, our aim was to select predictive marker genes for the GA combination drug in a simple and efficient manner. First, out of the 236 DEGs, we discarded genes with mRNA expression of less than 20, and secondly, the remaining genes were sorted in high order. Next, we narrowed down the gene list to 45 genes, which were then sorted in high order within each group. We then selected the top 10 genes from both the sensitive and resistant groups (Figure 8A). From the top 10 gene lists of the sensitive and resistant groups, we selected CRABP2 and IL4 as sensitive marker genes, and S100A4 and LPCAT1 as resistance marker genes (Figure 8B).

A.



B.

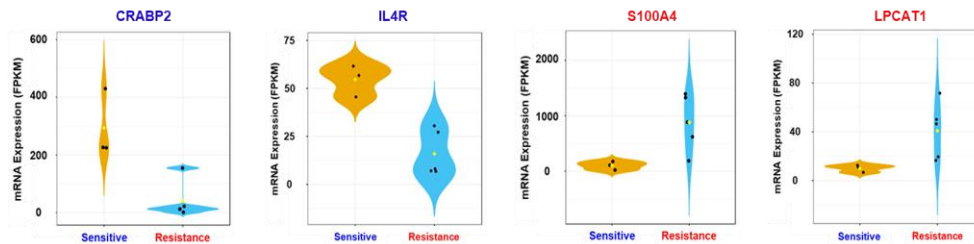


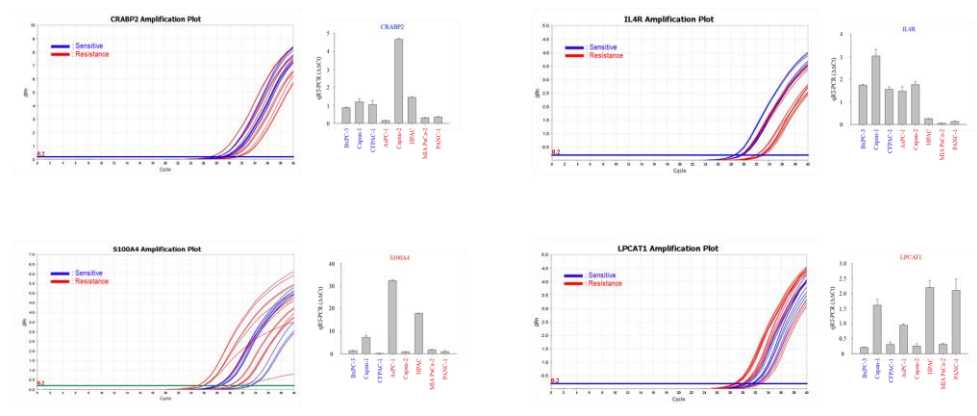
Figure 8. Predictive marker genes selection. (A) Heatmap of significantly expressed top 10 genes in sensitive and resistance groups. (B) Violin plots of the top 2 genes among the selected top 10 genes with each group. Red indicates upregulated genes, and green indicates downregulated genes in the heatmap. Orange represents the GA combination drug resistance group, and blue represents the GA combination drug sensitive group.

3.9. Confirmation of predictive marker genes mRNA expression using established pancreatic cancer cell line organoids

Subsequently, to identify CRABP2, IL4R, S100A4, and LPCAT1 genes for predicting the response to GA combination drug, we analyzed them using qRT-PCR (Figure 9A). PCR primers and conditions are presented in Table 1. To calculate between the predictive marker gene RNAseq (FPKM) and qRT-PCR ($\Delta\Delta Ct$), we observed the following results: IL4R had an R^2 value of 0.8448 and a p-value of 0.0012, S100A4 had an R^2 value of 0.5683 and a p-value of 0.031, LPCAT1 had an R^2 value of 0.1144 and a p-value of 0.7770, and CRABP2 had an R^2 value of 0.8448 and a p-value of 0.0012. When comparing the RNAseq (FPKM) and qRT-PCR ($\Delta\Delta Ct$) results of CRABP2, IL4R, S100A4, and LPCAT1, we found that IL4R, S100A4, and LPCAT1 RNAseq (FPKM) and qRT-PCR ($\Delta\Delta Ct$) results were correlated. However, CRABP2 RNAseq (FPKM) and qRT-PCR ($\Delta\Delta Ct$) results were inversely correlated (Figure 9B).

Based on these results, CRABP2 was not suitable as a predictive marker gene. Finally, we selected IL4R as a GA combination drug-sensitive predictive marker gene, and S100A4 and LPCAT1 were selected as resistance predictive marker genes.

A.



B.

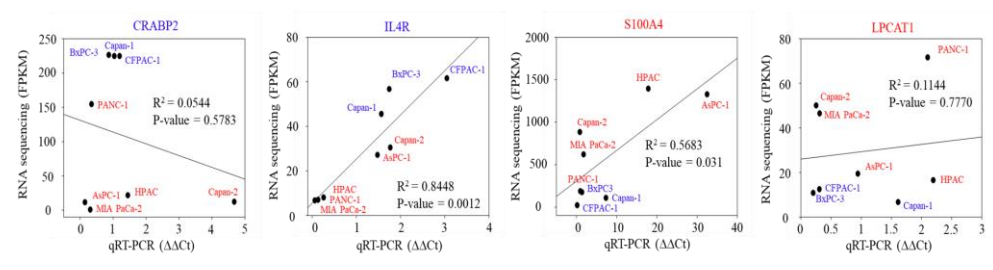


Figure 9. Correlation of mRNA expression between RNaseq and qRT-PCR. Amplification plot of selected 4 genes and $\Delta\Delta C_t$ values (A) and correlation plots between RNAseq (FPKM) and qRT-PCR $\Delta\Delta C_t$ (B). Red indicates GA combination drug-resistant genes and cell lines, and blue indicates GA combination drug-sensitive genes and cell lines.

Table 1. PCR primer sequences and conditions

1. PCR primer sequences						
Gene	Forward (5'-3')	Reverse (5'-3')	Amplicon (bp)	Accession no (NCBI)		
CRABP2	ATGAGACACCCGGATCATGT	CCCTCAAGTCCCCTTTAGAGAG	157	NM_001878.4		
IL4R	TACTTGCGAGTGGGAAGATGAAT	TATAGTTATCCGCACTGACCAC	172	NM_001257406.2		
S100A4	GGTGTCCACCTTCCACAAGT	GCTGTCCAAGTTGCTCATCA	154	NM_019554.3		
LPCAT1	ACCTATTCGAGCCATTGACC	CCTAATCCAGCTTCTTGCGAAC	233	NM_024830.5		
GAPDH	CAATGGAAATCCCATCACCA	ATGATGACCCTTTGGCTCC	161	NM_001357943.2		

2. PCR conditions						
Gene	Pre-denaturation	Denaturation	Annealing	Extension	Cycle	Final extension
CRABP2	95°C 5min	95°C 30sec	60°C 30sec	72°C 15sec	40 cycles	72°C 5min
IL4R	95°C 5min	95°C 30sec	60°C 30sec	72°C 15sec	40 cycles	72°C 5min
S100A4	95°C 5min	95°C 30sec	60°C 30sec	72°C 15sec	40 cycles	72°C 5min
LPCAT1	95°C 5min	95°C 30sec	60°C 30sec	72°C 20sec	40 cycles	72°C 5min
GAPDH	95°C 5min	95°C 30sec	60°C 30sec	72°C 15sec	40 cycles	72°C 5min

Abbreviation: PCR; Polymerase chain reaction, NCBI; National Center for Biotechnology Information, CRABP2; Cellular retinoic acid-binding protein 2, IL4R; Interleukin 4 receptor, LPCAT1; Lysophosphatidylcholine acyltransferase 1, S100A4; S100 calcium binding protein A4, GAPDH; Glyceraldehyde 3-phosphate dehydrogenase.

3.10. Confirmation of predictive marker genes protein expression using established pancreatic cancer cell line organoids

To confirm GA predictive marker genes at the protein level, we analyzed them using Western blot (Figure 10A) and IHC (Figure 10B) in established pancreatic cancer cell line organoids. The pancreatic cancer cell line organoids GA IC50, IHC H-score of IL4R, S100A4 and LPCAT1 are presented in Table 2. To calculate the relationship between the protein expression of the predictive marker genes (IHC H-score) and the GA combination drug IC50 in pancreatic cancer cell line organoids, we observed the following results: IL4R had an R^2 value of 0.4426 and a p-value of 0.0717, S100A4 had an R^2 value of 0.5505 and a p-value of 0.0351, and LPCAT1 had an R^2 value of 0.0001 and a p-value of 0.9785. We found that the IL4R IHC H-score area was inversely correlated, while the S100A4 IHC-positive area was correlated with the GA combination drug IC50 (Figure 10C). Despite the correlation between the LPCAT1 positive area and IC50, the low R^2 value and high p-value indicated that LPCAT1 was not suitable as a predictive marker gene.

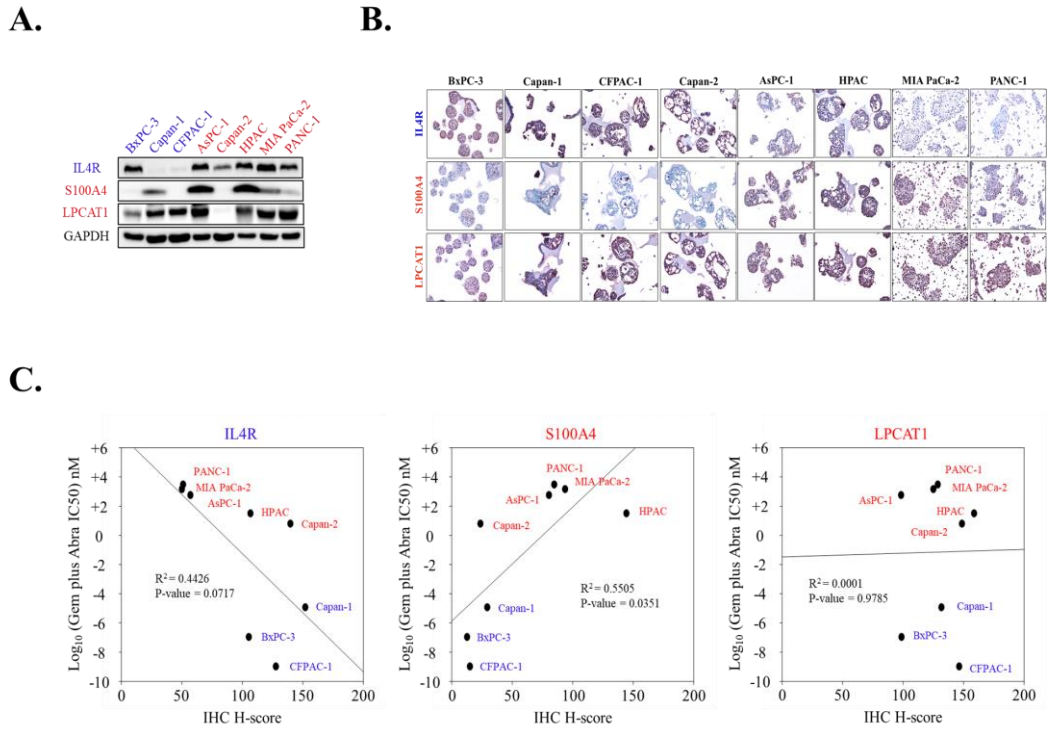


Figure 10. Confirmation of GA combination drug predictive marker genes protein expression.

Confirmation of predictive marker genes IL4R, S100A4 and LPCAT1 protein expression using western blot (A) and IHC; Light blue, Hematoxylin staining shows the nucleus; Dark brown, DAB staining shows the presence of IL4R, S100A4 and LPCAT1 (B). Correlation between IHC and GA combination drug sensitivity (C). Red indicates GA combination drug-resistant genes and cell lines, and blue indicates GA combination drug-sensitive genes and cell lines.

Table 2. Comparison of GA combination drug predictive marker genes IHC H-score in established pancreatic cancer cell line ornaoids

Cell lines	Log ₁₀ (GA IC50) nM	Response	IHC H-score		
			IL4R	S100A4	LPCAT1
AsPC-1	2.8	Resistance	57.0	58.5	98.3
BxPC-3	-7.0	Sensitive	105.3	14.3	98.7
Capan-1	-4.9	Sensitive	152.0	23.9	131.7
Capan-2	0.8	Resistance	139.7	25.0	148.7
CFPAC-1	-9.0	Sensitive	127.7	11.3	146.3
HPAC	1.5	Resistance	106.7	84.3	158.7
MiaPaCa-2	3.2	Resistance	50.0	67.7	125.0
PANC-1	3.5	Resistance	51.0	71.3	128.7

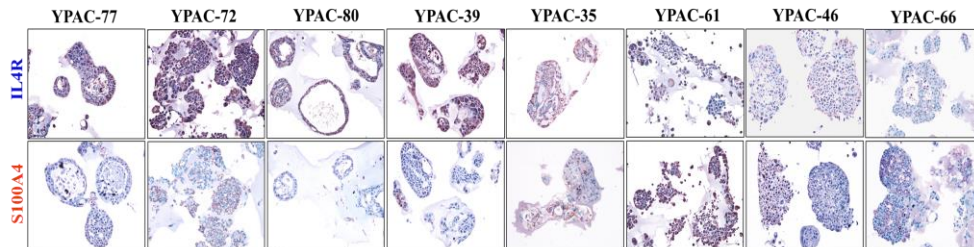
Abbreviation: GA; Gemcitabine plus Abraxane (nab-paclitaxel) combination drug, IC50; Inhibition concentration 50, IHC; Immunohistochemistry, H-score; Histoscore, IL4R; Interleukin 4 receptor, S100A4; S100 calcium binding protein A4.

3.11. Validation of predictive marker genes using established CRC YPAC cell line organoids

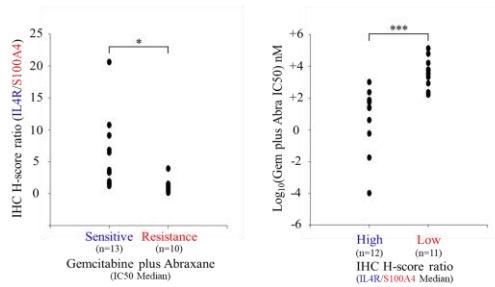
To validate GA predictive marker genes at the protein level, we first analyzed them using IHC in established CRC YPAC cell line organoids (Figure 11A). Second, CRC YPAC organoids were divided into two groups: sensitive (GA combination drug IC50 < Median, n=13) and resistant (GA combination drug IC50 > Median, n=10). Third, we calculated the IL4R/S100A4 H-score ratio median for the sensitive and resistant groups. Based on this median, CRC YPAC organoids were divided into two groups: high (IL4R/S100A4 H-score ratio > Median, n=12) and low (IL4R/S100A4 H-score ratio < Median, n=11). The high group was considered sensitive and the low group was considered resistant. The CRC YPAC cell line organoids GA IC50, IHC H-score of S100A4 and IL4R, IL4R/S100A4 ratio, group, response, prediction, and match are presented in Table 3. Using this classification to predict GA sensitivity in the high group (n=12) and low group (n=11) of CRC YPAC cell line organoids, we were able to predict GA sensitivities for 20 out of 23 samples (87 %). To calculate the p-value between the high and low group's GA IC50, we observed the following results: the high and low groups had a p-value of 0.0004. IHC analysis revealed that the IL4R IHC positive area was inversely correlated with the GA combination drug IC50, while the S100A4 IHC positive area was positively correlated (Figure 11B). Finally, by analyzing how the difference in expression of IL4R and S100A4 affects the patient's overall survival, it was confirmed that overall survival was higher when the expression of S100A4 was low and the expression of IL4R was high (Figure 11C).

These results confirmed that IL4R protein expression was inversely correlated with GA combination drug IC50, while S100A4 protein expression was positively correlated with GA combination drug IC50 in CRC YPAC cell line organoids. Based on this research, we suggest that IL4R can be utilized as a sensitivity marker and S100A4 as a resistance marker for the GA combination drug in pancreatic cancer.

A.



B.



C.

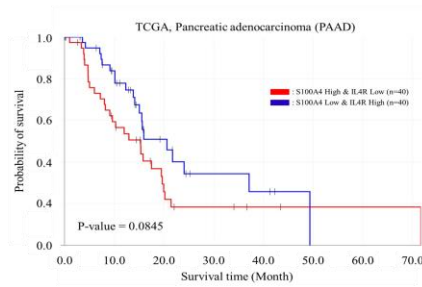


Figure 11. IL4R and S100A4 IHC and IC50 values of GA combination drug in established CRC YPAC cell line organoids. (A) Positive rate of IL4R and S100A4 protein expression showed negative correlation using IHC staining; Light blue, Hematoxylin staining shows the nucleus; Dark brown, DAB staining shows the presence of IL4R and S100A4. (B) IC50 values for GA combination drug. Asterisks (***) indicate statistical significances at p-value <0.001 and (*) indicate statistical significances at p-value <0.05. (C) Kaplan-Meier survival curves of pancreatic adenocarcinoma patients' overall survival (OS) were analyzed between two groups: S100A4 high & IL4R low, and S100A4 low & IL4R high, using data from TCGA.

Table 3. Comparison of GA combination drug predictive marker genes IHC H-score in established CRC YPAC cell line orgnaoids

Cell lines	Log ₁₀ (GA IC50) nM	Response	IHC H-score				Group	Prediction	Outcome
			S100A4	IL4R	IL4R / S100A4				
YPAC-02	4.2	Resistance	61.1	65.7	1.20	Low	Resistance	O	
YPAC-05	1.9	Sensitive	15.3	77.3	6.84	High	Sensitive	O	
YPAC-17	1.9	Sensitive	29.8	74.9	3.33	High	Sensitive	O	
YPAC-23	2.9	Resistance	65.5	66.3	0.93	Low	Resistance	O	
YPAC-27	-1.8	Sensitive	60.4	87.5	1.93	High	Sensitive	O	
YPAC-28	5.1	Resistance	57.1	68.3	1.44	Low	Resistance	O	
YPAC-29	2.4	Sensitive	63.3	78.3	1.53	Low	Resistance	X	
YPAC-31	2.4	Sensitive	7.2	48.6	9.11	High	Sensitive	O	
YPAC-35	3.3	Resistance	38.0	36.7	1.09	Low	Resistance	O	
YPAC-39	1.4	Sensitive	36.8	62.4	3.28	High	Sensitive	O	
YPAC-43	2.2	Sensitive	60.0	64.2	1.20	Low	Resistance	X	
YPAC-46	3.8	Resistance	59.3	46.2	0.72	Low	Resistance	O	
YPAC-47	3.8	Resistance	24.4	7.1	0.38	Low	Resistance	O	
YPAC-52	0.6	Sensitive	14.9	23.6	1.58	High	Sensitive	O	
YPAC-57	1.8	Sensitive	2.1	30.7	20.60	High	Sensitive	O	
YPAC-58	1.7	Sensitive	7.5	59.3	10.74	High	Sensitive	O	
YPAC-61	3.6	Resistance	65.3	50.3	0.61	Low	Resistance	O	
YPAC-66	4.8	Resistance	41.4	6.4	0.14	Low	Resistance	O	
YPAC-67	3.0	Resistance	9.1	31.3	3.92	High	Sensitive	X	
YPAC-72	-0.2	Sensitive	18.3	70.8	6.44	High	Sensitive	O	
YPAC-77	-4.0	Sensitive	40.6	64.8	1.67	High	Sensitive	O	
YPAC-79	3.5	Resistance	35.8	50.6	1.52	Low	Resistance	O	
YPAC-80	1.4	Sensitive	15.5	48.8	3.69	High	Sensitive	O	

Abbreviation: GA; Gemcitabine plus Abraxane (nab-paclitaxel) combination drug, IC50; Inhibition concentration 50, IHC; Immunohistochemistry, H-score; HistoScore, IL4R; Interleukin 4 receptor, S100A4; S100 calcium binding protein A4.

4. DISCUSSION

In pancreatic cancer, more than 80% of patients have advanced cancer that cannot be surgically resected.^{3,4} Therefore, the discovery of biomarkers for selecting anticancer drugs based on FOLFIRINOX (5-fluorouracil, folinic acid, irinotecan, oxaliplatin) and gemcitabine-based anticancer drug, which are currently used as primary standard treatments, is crucial. However, there are still no standards or biomarkers to determine which patients should choose between FOLFIRINOX and gemcitabine-based anticancer drugs as their primary treatment for pancreatic cancer.^{33,34} The discovery of biomarkers to guide the selection of FOLFIRINOX or gemcitabine-based anticancer drugs is of great significance for improving the average patient's survival time.

In particular, for pancreatic cancer organoids, organoid culture media typically contain Wnt3a, Noggin, and R-spondin. Specifically, Wnt3a is an essential component for the Wnt signaling pathway in cancer and plays a major role in organoid culture.⁵⁵⁻⁵⁹ However, Wnt3a has an insoluble domain, causing aggregation in the culture media, and this aggregated Wnt3a induces organoid growth obstruction.⁶⁰ To solve this problem, several studies have found that afamin can maintain Wnt3a activity,⁶¹⁻⁶⁷ but Wnt3a/afamin organoid culture media costs twice as much as existing organoid culture media, making Wnt3a/afamin organoid culture media unsuitable for our laboratory.

To find an alternative way to solve this problem, several studies used normal cell culture media for organoid culture.^{21,24} Based on these studies, we used normal cell culture media for pancreatic cancer cell line organoid culture and F-media for CRC YPAC cell line organoid culture, without using organoid culture media. We successfully established pancreatic cancer cell line organoids in normal cell culture media condition and CRC YPAC cell line organoids in F-media culture condition, without using organoid culture media. Notably, the CRC YPAC cell line organoid exhibits histological characteristics similar to primary tumor tissues. Furthermore, we compared the sensitivity of anticancer drugs to GA combination therapy through the 3D organoid drug test platform established using the matrigel-based 3D organoid culture model. This platform accurately reflects the clinical results of patients who received GA combination chemotherapy, which has not yet been published.

To identify marker genes that can predict the effectiveness of the GA combination drug, the analysis was conducted by dividing the pancreatic cancer cell lines into a sensitive group and a resistant group based on the IC50 results of 8 pancreatic cancer cell line organoids treated with the GA

combination drug. As a result, we identified IL4R as the sensitivity marker gene for the GA combination drug, and S100A4 as the resistance marker gene. We compared the protein expression of IL4R and S100A4 with the IC50 of GA combination drug in CRC YPAC cell line organoids. Higher protein expression of IL4R indicated greater sensitivity to the GA combination drug. Conversely, higher protein expression of S100A4 indicated greater resistance to the GA combination drug. Through the above results, it was confirmed that IL4R can be used as the sensitivity marker gene for the GA combination drug, and S100A4 can be used as the resistance marker gene.

Interleukin-4 receptor (IL4R) is a receptor of Interleukin-4 (IL4) secreted by T helper 2 cells (Th2 cells) that is involved in the regulation of the immune response and the growth of tumors.⁶⁸⁻⁷⁰ The expression of IL4R is increased in pancreatic cancer cell lines and tumor tissues of pancreatic cancer patients.⁶⁸⁻⁷² Research is currently underway on the role of the IL4R complex in cancer progression. Among the findings, the expression of IL4R type 2, consisting of IL4R α and IL13R α 1, is increased in solid tumors and fibroblasts, and is associated with poor prognosis in pancreatic cancer. IL4R type 1, consisting of IL4R α and IL13R γ c, is increased in T cells and NK cells.^{73,74} Recently, there have been research results indicating that targeting IL4R in pancreatic cancer can effectively overcome tumor immunity and suppress tumor growth and metastasis.^{75,76} However, additional research is needed to determine whether IL4R directly or indirectly influences the mechanism of action for GA combination drug.

S100A4 was highly expressed in pancreatic cancer and confirmed as a predictor of early recurrence in PDAC patients.^{77,78} Additionally, knockdown of S100A4 increases the sensitivity of pancreatic cancer cell lines to gemcitabine.⁷⁹ S100A4 can also be combined with other tumor biomarkers for the diagnosis, prognosis, and chemo-response of PDAC.⁸⁰⁻⁸² S100A4 promotes the tumor cell migration phenotype, and decreased S100A4 not only reduces tumor cell migration but also inhibits tumor cell EMT, according to several studies.⁸³⁻⁸⁶ Therefore, S100A4 can be used as an effective biomarker for early diagnosis of cancer and prediction of cancer metastasis. In addition, extracellular S100A4 is released into blood plasma in the form of multimeric protein,⁸³ and S100A4 is included among niches known to promote metastasis in oncogenic exosomes.⁸⁷ In this study, it was confirmed that S100A4 could be used as a resistance marker for GA combination drug, but the direct or indirect mechanism between S100A4 and GA combination drug was not confirmed. However, studies have shown that exosomes secreted from donor cells of pancreatic cancer perform the function of cargo and increase resistance to gemcitabine and Abraxane (nab-paclitaxel) in recipient cells.⁸⁸ Therefore,

the release of S100A4 can increase resistance to gemcitabine plus Abraxane (nab-paclitaxel) combination drug. If this process is suppressed, a high therapeutic effect of gemcitabine plus Abraxane (nab-paclitaxel) combination drug can be expected.

Recently, in pancreatic cancer, patient survival and response to chemotherapy have been found to depend on the molecular subtypes of the cancer. Two major molecular subtypes of pancreatic cancer have been reported: the classical type and the basal-like type.⁸⁹⁻⁹² In addition, studies on patient prognosis prediction and treatment response were conducted based on two subtypes of pancreatic cancer. It was confirmed that the prognosis was relatively worse for patients with the basal-like type compared to those with the classical type, and that effective anticancer drug differed between the classical and basal-like types.^{93,94} Furthermore, a single-cell transcript analysis conducted using tissues from 17 pancreatic cancer patients in the laboratory recently confirmed that pancreatic cancer cells can be divided into a total of six molecular biological subtypes, including the previously reported classical type and basal-like type. Each molecular biological subtype can be distinguished by the expression of three or four characteristic marker genes.⁹⁵ In particular, in this study, S100A4, which was selected as the resistance marker gene for the GA combination drug, is one of several marker genes of the basal-like type in pancreatic cancer⁹⁵ and breast cancer.^{96,97} There is evidence that the classical type is relatively more effective against gemcitabine-based anticancer drug than the basal-like type. Based on this, it can be suggested that S100A4 may be used as a resistance marker gene for the GA combination drug. However, considering the characteristics of the tumor microenvironment, where pancreatic cancer cells and various surrounding cells are mixed, predicting the response to GA combination drug on the expression of a single gene, S100A4, is limited. Therefore, it is necessary to use S100A4 in combination with other marker genes as a biomarker for selecting chemotherapy and to verify its effectiveness through retrospective analysis to more accurately predict the response to GA combination drug.

Also, in pancreatic cancer, cancer-associated fibroblasts (CAFs) have been associated with chemoresistance. Targeting CAFs in pancreatic ductal adenocarcinoma (PDAC) has become a potential therapeutic strategy for pancreatic cancer.⁹⁸⁻¹⁰³ Specifically, in pancreatic cancer organoids with CAFs co-culture condition, pancreatic cancer organoid proliferation increased and chemo-induced cell death decreased.¹⁰⁴ S100A4 and IL4R were expressed not only in the tumor but also in CAFs. Especially, monoclonal antibodies are especially useful as delivery tools for directing drugs directly to the tumor site or tumor microenvironment (TME). They enhance on-target tumor killing,

induce immune cell responses, and reduce the side effects of chemotherapy. Using this approach, antibody-drug conjugates (ADCs) are considered one of the best options.^{105,106} Several studies on pancreatic cancer have ADCs as potential strategies to improve and induce effective therapy.¹⁰⁷⁻¹¹⁰ Therefore, S100A4 and IL4R-targeted therapy may show a synergistic effect when combined with GA in the treatment of pancreatic cancer.

There are several limitations in this study. The first limitation is the number of pancreatic cancer cell lines used in the analysis. In this study, when 8 pancreatic cancer cell lines were divided into a sensitive group and a resistant group based on sensitivity to GA combination drug, BxPC-3, Capan-1, and CFPAC-1 were categorized as the sensitive group, while AsPC-1, Capan-2, HPAC, MIA PaCa-2, and PANC-1 were categorized as the resistant group. The number of cell lines included in the sensitive group was less than that of the resistant group, resulting in an unequal ratio. In addition, the limited number of 8 pancreatic cancer cell lines used in the analysis could lead to a large margin of error, making accurate analysis difficult. To compensate for this, a more accurate analysis could be conducted by measuring the sensitivity to GA combination drug through the same process and reducing the error by matching the ratio of the sensitive group and the resistant group. The second limitation is that the pancreatic cancer cell line used to find the predictive marker gain for GA combination drug is not a primary cancer cell line but a commercial cell line. Commercial cell lines, while originating from actual patients, are artificially induced to have various genetic mutations for experimental convenience, causing some of their unique characteristics to be lost. Therefore, when comparing the results in the CRC YPAC cell line established in the laboratory (Figure 10C, E), the expected pattern was found for the sensitive marker gene IL4R and the resistance marker gene S100A4. However, the results were not as robust as those obtained with the commercial cell line. To address this, it is suggested that a marker gain which can more accurately predict the effect on the CRC YPAC cell line could be selected based on clinical information and the results of sensitivity tests using GA combination drug on a matrigel-based 3D organoid drug test platform established in this study.

5. CONCLUSION

In this study, we aimed to enhance the therapeutic effect against pancreatic cancer by identifying predictive marker genes for the efficacy of the gemcitabine plus Abraxane (nab-paclitaxel) combination drug. We established a matrigel-based 3D organoid culture model and drug test platform using pancreatic cancer cell lines in normal cell culture media condition and patient-derived pancreatic cancer cells (CRC YPAC cell lines) in F-media condition, without using organoid culture media. Utilizing organoid culture model and drug test platform, we identified IL4R as a sensitivity marker and S100A4 as a resistance marker for the gemcitabine plus Abraxane (nab-paclitaxel) combination drug. However, since this study was conducted using a limited number of samples, further research with a larger sample size is needed for clinical significance. Additionally, research on the molecular biological mechanisms involving IL4R and S100A4, which are not yet fully understood, is also necessary.

References

1. Siegel RL, Miller KD, Wagle NS, Jemal A. Cancer statistics, 2023. *CA Cancer J Clin* 2023;73:17-48.
2. Rahib L, Wehner MR, Matrisian LM, Nead KT. Estimated Projection of US Cancer Incidence and Death to 2040. *JAMA Netw Open* 2021;4:e214708.
3. Conroy T, Desseigne F, Ychou M, Bouché O, Guimbaud R, Bécouarn Y, et al. FOLFIRINOX versus Gemcitabine for Metastatic Pancreatic Cancer. *New England Journal of Medicine* 2011;364:1817-25.
4. Tempero MA, Malafa MP, Al-Hawary M, Behrman SW, Benson AB, Cardin DB, et al. Pancreatic Adenocarcinoma, Version 2.2021, NCCN Clinical Practice Guidelines in Oncology. *J Natl Compr Canc Netw* 2021;19:439-57.
5. Von Hoff DD, Ervin T, Arena FP, Chiorean EG, Infante J, Moore M, et al. Increased Survival in Pancreatic Cancer with nab-Paclitaxel plus Gemcitabine. *New England Journal of Medicine* 2013;369:1691-703.
6. Gillet JP, Varma S, Gottesman MM. The clinical relevance of cancer cell lines. *J Natl Cancer Inst* 2013;105:452-8.
7. Mizushima H, Wang X, Miyamoto S, Mekada E. Integrin signal masks growth-promotion activity of HB-EGF in monolayer cell cultures. *J Cell Sci* 2009;122:4277-86.
8. Huang GS, Tseng TC, Dai NT, Fu KY, Dai LG, Hsu SH. Fast isolation and expansion of multipotent cells from adipose tissue based on chitosan-selected primary culture. *Biomaterials* 2015;65:154-62.
9. Gurski LA, Petrelli NJ, Jia X, Farach-Carson MC. 3D Matrices for Anti-Cancer Drug Testing and Development. *Oncology Issues* 2010;25:20-5.
10. Drost J, Clevers H. Organoids in cancer research. *Nat Rev Cancer* 2018;18:407-18.
11. Wu M-H, Chang Y-H, Liu Y-T, Chen Y-M, Wang S-S, Wang H-Y, et al. Development of high throughput microfluidic cell culture chip for perfusion 3-dimensional cell culture-based chemosensitivity assay. *Sensors and Actuators B: Chemical* 2011;155:397-407.
12. Gurski LA, Jha AK, Zhang C, Jia X, Farach-Carson MC. Hyaluronic acid-based hydrogels as 3D matrices for in vitro evaluation of chemotherapeutic drugs using poorly adherent prostate cancer cells. *Biomaterials* 2009;30:6076-85.

13. Abbas ZN, Al-Saffar AZ, Jasim SM, Sulaiman GM. Comparative analysis between 2D and 3D colorectal cancer culture models for insights into cellular morphological and transcriptomic variations. *Sci Rep* 2023;13:18380.
14. Shichi Y, Sasaki N, Michishita M, Hasegawa F, Matsuda Y, Arai T, et al. Enhanced morphological and functional differences of pancreatic cancer with epithelial or mesenchymal characteristics in 3D culture. *Sci Rep* 2019;9:10871.
15. Minami F, Sasaki N, Shichi Y, Gomi F, Michishita M, Ohkusu-Tsukada K, et al. Morphofunctional analysis of human pancreatic cancer cell lines in 2- and 3-dimensional cultures. *Sci Rep* 2021;11:6775.
16. Lawrenson K, Notaridou M, Lee N, Benjamin E, Jacobs IJ, Jones C, Gayther SA. In vitro three-dimensional modeling of fallopian tube secretory epithelial cells. *BMC Cell Biology* 2013;14:43.
17. Lv D, Hu Z, Lu L, Lu H, Xu X. Three-dimensional cell culture: A powerful tool in tumor research and drug discovery. *Oncol Lett* 2017;14:6999-7010.
18. Law AMK, Rodriguez de la Fuente L, Grundy TJ, Fang G, Valdes-Mora F, Gallego-Ortega D. Advancements in 3D Cell Culture Systems for Personalizing Anti-Cancer Therapies. *Front Oncol* 2021;11:782766.
19. Lee DW, Choi YS, Seo YJ, Lee MY, Jeon SY, Ku B, Nam DH. High-throughput, miniaturized clonogenic analysis of a limiting dilution assay on a micropillar/microwell chip with brain tumor cells. *Small* 2014;10:5098-105.
20. Lancaster MA, Knoblich JA. Organogenesis in a dish: modeling development and disease using organoid technologies. *Science* 2014;345:1247125.
21. Oz O, Iscan E, Batur T, Ozturk M. 3D Organoid modelling of hepatoblast-like and mesenchymal-like hepatocellular carcinoma cell lines. *Hepatoma Research* 2021; doi:10.20517/2394-5079.2021.43.
22. Osuna de la Pena D, Trabulo SMD, Collin E, Liu Y, Sharma S, Tatari M, et al. Bioengineered 3D models of human pancreatic cancer recapitulate in vivo tumour biology. *Nat Commun* 2021;12:5623.
23. Park SJ, Yoo HC, Ahn E, Luo E, Kim Y, Sung Y, et al. Enhanced Glutaminolysis Drives Hypoxia-Induced Chemoresistance in Pancreatic Cancer. *Cancer Res* 2023;83:735-52.
24. Nelson SR, Zhang C, Roche S, O'Neill F, Swan N, Luo Y, et al. Modelling of pancreatic

- cancer biology: transcriptomic signature for 3D PDX-derived organoids and primary cell line organoid development. *Scientific Reports* 2020;10.
25. LeSavage BL, Suhar RA, Broguiere N, Lutolf MP, Heilshorn SC. Next-generation cancer organoids. *Nat Mater* 2022;21:143-59.
 26. Boj SF, Hwang CI, Baker LA, Chio, II, Engle DD, Corbo V, et al. Organoid models of human and mouse ductal pancreatic cancer. *Cell* 2015;160:324-38.
 27. Karthaus WR, Iaquina PJ, Drost J, Gracanin A, van Boxtel R, Wongvipat J, et al. Identification of multipotent luminal progenitor cells in human prostate organoid cultures. *Cell* 2014;159:163-75.
 28. Huch M, Gehart H, van Boxtel R, Hamer K, Blokzijl F, Verstegen MM, et al. Long-term culture of genome-stable bipotent stem cells from adult human liver. *Cell* 2015;160:299-312.
 29. Bartfeld S, Bayram T, van de Wetering M, Huch M, Begthel H, Kujala P, et al. In vitro expansion of human gastric epithelial stem cells and their responses to bacterial infection. *Gastroenterology* 2015;148:126-36 e6.
 30. Rock JR, Onaitis MW, Rawlins EL, Lu Y, Clark CP, Xue Y, et al. Basal cells as stem cells of the mouse trachea and human airway epithelium. *Proceedings of the National Academy of Sciences* 2009;106:12771-5.
 31. Sachs N, de Ligt J, Kopper O, Gogola E, Bounova G, Weeber F, et al. A Living Biobank of Breast Cancer Organoids Captures Disease Heterogeneity. *Cell* 2018;172:373-86 e10.
 32. Gao D, Vela I, Sboner A, Iaquina PJ, Karthaus WR, Gopalan A, et al. Organoid cultures derived from patients with advanced prostate cancer. *Cell* 2014;159:176-87.
 33. Uzunparmak B, Sahin IH. Pancreatic cancer microenvironment: a current dilemma. *Clin Transl Med* 2019;8:2.
 34. Mizrahi JD, Surana R, Valle JW, Shroff RT. Pancreatic cancer. *The Lancet* 2020;395:2008-20.
 35. Lee HS, Lee JS, Lee J, Kim EK, Kim H, Chung MJ, et al. Establishment of pancreatic cancer cell lines with endoscopic ultrasound-guided biopsy via conditionally reprogrammed cell culture. *Cancer Medicine* 2019;8:3339-48.
 36. Lee HS, Kim E, Lee J, Park SJ, Hwang HK, Park CH, et al. Profiling of conditionally reprogrammed cell lines for in vitro chemotherapy response prediction of pancreatic cancer.

- EBioMedicine 2021;65:103218.
37. Broutier L, Andersson-Rolf A, Hindley CJ, Boj SF, Clevers H, Koo BK, Huch M. Culture and establishment of self-renewing human and mouse adult liver and pancreas 3D organoids and their genetic manipulation. *Nat Protoc* 2016;11:1724-43.
 38. Driehuis E, Gracanin A, Vries RGJ, Clevers H, Boj SF. Establishment of Pancreatic Organoids from Normal Tissue and Tumors. *STAR Protoc* 2020;1:100192.
 39. Zhang SW, Chen W, Lu XF, Wen Z, Hu L, Liu YH, et al. An efficient and user-friendly method for cytohistological analysis of organoids. *J Tissue Eng Regen Med* 2021;15:1012-22.
 40. Worsdorfer P, Rockel A, Alt Y, Kern A, Ergun S. Generation of Vascularized Neural Organoids by Co-culturing with Mesodermal Progenitor Cells. *STAR Protoc* 2020;1:100041.
 41. Zaqout S, Becker LL, Kaindl AM. Immunofluorescence Staining of Paraffin Sections Step by Step. *Front Neuroanat* 2020;14:582218.
 42. Choi SJ, Choi YI, Kim L, Park IS, Han JY, Kim JM, Chu YC. Preparation of compact agarose cell blocks from the residues of liquid-based cytology samples. *Korean J Pathol* 2014;48:351-60.
 43. Li Z, Yu L, Chen D, Meng Z, Chen W, Huang W. Protocol for generation of lung adenocarcinoma organoids from clinical samples. *STAR Protoc* 2021;2:100239.
 44. Bergdorf K, Phifer C, Bharti V, Westover D, Bauer J, Vilgelm A, et al. High-throughput drug screening of fine-needle aspiration-derived cancer organoids. *STAR Protoc* 2020;1:100212.
 45. Calandrini C, Drost J. Normal and tumor-derived organoids as a drug screening platform for tumor-specific drug vulnerabilities. *STAR Protoc* 2022;3:101079.
 46. Larsen BM, Cancino A, Shaxted JM, Salahudeen AA. Protocol for drug screening of patient-derived tumor organoids using high-content fluorescent imaging. *STAR Protoc* 2022;3:101407.
 47. Maenhoudt N, Vankelecom H. Protocol for establishing organoids from human ovarian cancer biopsies. *STAR Protoc* 2021;2:100429.
 48. Fujii E, Yamazaki M, Kawai S, Ohtani Y, Watanabe T, Kato A, Suzuki M. A simple method for histopathological evaluation of organoids. *J Toxicol Pathol* 2018;31:81-5.

49. Shichi Y, Gomi F, Sasaki N, Nonaka K, Arai T, Ishiwata T. Epithelial and Mesenchymal Features of Pancreatic Ductal Adenocarcinoma Cell Lines in Two- and Three-Dimensional Cultures. *J Pers Med* 2022;12.
50. Creation of Efficient Pathology Research Pipelines for Discovery: Tissue Microarray Construction Coupled with Digital Image Analysis. *Journal of Clinical and Translational Pathology* 2021; doi:10.14218/jctp.2021.00012.
51. Werry J-E, Müller S, Wehrhan F, Geppert C, Frohwitter G, Ries J, et al. Accuracy Analysis of a Next-Generation Tissue Microarray on Various Soft Tissue Samples of Wistar Rats. *Applied Sciences* 2021;11.
52. Kim KH, Choi SJ, Choi YI, Kim L, Park IS, Han JY, et al. In-house Manual Construction of High-Density and High-Quality Tissue Microarrays by Using Homemade Recipient Agarose-Paraffin Blocks. *Korean J Pathol* 2013;47:238-44.
53. Li JS, Tang PC, Choi CKK, Chan AS, Ng CS, To KF, Tang PM. Protocol to study immunodynamics in the tumor microenvironment using a tyramide signal amplification-based immunofluorescent multiplex panel. *STAR Protoc* 2024;5:102823.
54. Longati P, Jia X, Eimer J, Wagman A, Witt M-R, Rehnmark S, et al. 3D pancreatic carcinoma spheroids induce a matrix-rich, chemoresistant phenotype offering a better model for drug testing. *BMC Cancer* 2013;13:95.
55. Shi X, Li Y, Yuan Q, Tang S, Guo S, Zhang Y, et al. Integrated profiling of human pancreatic cancer organoids reveals chromatin accessibility features associated with drug sensitivity. *Nat Commun* 2022;13:2169.
56. Balak JRA, Juksar J, Carlotti F, Lo Nigro A, de Koning EJP. Organoids from the Human Fetal and Adult Pancreas. *Curr Diab Rep* 2019;19:160.
57. Sereti E, Papapostolou I, Dimas K. Pancreatic Cancer Organoids: An Emerging Platform for Precision Medicine? *Biomedicines* 2023;11.
58. Casamitjana J, Espinet E, Rovira M. Pancreatic Organoids for Regenerative Medicine and Cancer Research. *Front Cell Dev Biol* 2022;10:886153.
59. Huch M, Bonfanti P, Boj SF, Sato T, Loomans CJ, van de Wetering M, et al. Unlimited in vitro expansion of adult bi-potent pancreas progenitors through the Lgr5/R-spondin axis. *EMBO J* 2013;32:2708-21.
60. Mihara E, Hirai H, Yamamoto H, Tamura-Kawakami K, Matano M, Kikuchi A, et al. Active

and water-soluble form of lipidated Wnt protein is maintained by a serum glycoprotein afamin/alpha-albumin. *Elife* 2016;5.

61. Roe JS, Hwang CI, Somerville TDD, Milazzo JP, Lee EJ, Da Silva B, et al. Enhancer Reprogramming Promotes Pancreatic Cancer Metastasis. *Cell* 2017;170:875-88 e20.
62. Ikezawa K, Ekawa T, Hasegawa S, Kai Y, Takada R, Yamai T, et al. Establishment of organoids using residual samples from saline flushes during endoscopic ultrasound-guided fine-needle aspiration in patients with pancreatic cancer. *Endosc Int Open* 2022;10:E82-E7.
63. Seino T, Kawasaki S, Shimokawa M, Tamagawa H, Toshimitsu K, Fujii M, et al. Human Pancreatic Tumor Organoids Reveal Loss of Stem Cell Niche Factor Dependence during Disease Progression. *Cell Stem Cell* 2018;22:454-67 e6.
64. Miyabayashi K, Baker LA, Deschenes A, Traub B, Caligiuri G, Plenker D, et al. Intraductal Transplantation Models of Human Pancreatic Ductal Adenocarcinoma Reveal Progressive Transition of Molecular Subtypes. *Cancer Discov* 2020;10:1566-89.
65. Tiriach H, Belleau P, Engle DD, Plenker D, Deschenes A, Somerville TDD, et al. Organoid Profiling Identifies Common Responders to Chemotherapy in Pancreatic Cancer. *Cancer Discov* 2018;8:1112-29.
66. Farshadi EA, Chang J, Sampadi B, Doukas M, Van 't Land F, van der Sijde F, et al. Organoids Derived from Neoadjuvant FOLFIRINOX Patients Recapitulate Therapy Resistance in Pancreatic Ductal Adenocarcinoma. *Clin Cancer Res* 2021;27:6602-12.
67. Tiriach H, Bucobo JC, Tzimas D, Grewel S, Lacombe JF, Rowehl LM, et al. Successful creation of pancreatic cancer organoids by means of EUS-guided fine-needle biopsy sampling for personalized cancer treatment. *Gastrointest Endosc* 2018;87:1474-80.
68. Kawakami K, Kawakami M, Husain SR, Puri RK. Targeting interleukin-4 receptors for effective pancreatic cancer therapy. *Cancer Res* 2002;62:3575-80.
69. Shi J, Song X, Traub B, Luxenhofer M, Kornmann M. Involvement of IL-4, IL-13 and Their Receptors in Pancreatic Cancer. *Int J Mol Sci* 2021;22.
70. Prokopchuk O, Liu Y, Henne-Bruns D, Kornmann M. Interleukin-4 enhances proliferation of human pancreatic cancer cells: evidence for autocrine and paracrine actions. *Br J Cancer* 2005;92:921-8.
71. Suzuki A, Leland P, Joshi BH, Puri RK. Targeting of IL-4 and IL-13 receptors for cancer therapy. *Cytokine* 2015;75:79-88.

72. Shimamura T, Royal RE, Kioi M, Nakajima A, Husain SR, Puri RK. Interleukin-4 cytotoxin therapy synergizes with gemcitabine in a mouse model of pancreatic ductal adenocarcinoma. *Cancer Res* 2007;67:9903-12.
73. Kim KM, Hussein UK, Park SH, Moon YJ, Zhang Z, Ahmed AG, et al. Expression of IL4Ralpha and IL13Ralpha1 are associated with poor prognosis of soft-tissue sarcoma of the extremities, superficial trunk, and retroperitoneum. *Diagn Pathol* 2021;16:2.
74. Dey P, Li J, Zhang J, Chaurasiya S, Strom A, Wang H, et al. Oncogenic KRAS-Driven Metabolic Reprogramming in Pancreatic Cancer Cells Utilizes Cytokines from the Tumor Microenvironment. *Cancer Discov* 2020;10:608-25.
75. Zhou Y, Farooq MA, Ajmal I, He C, Gao Y, Guo D, et al. Co-expression of IL-4/IL-15-based inverted cytokine receptor in CAR-T cells overcomes IL-4 signaling in immunosuppressive pancreatic tumor microenvironment. *Biomed Pharmacother* 2023;168:115740.
76. Vadevoo SMP, Kang Y, Gunassekaran GR, Lee SM, Park MS, Jo DG, et al. IL4 receptor targeting enables nab-paclitaxel to enhance reprogramming of M2-type macrophages into M1-like phenotype via ROS-HMGB1-TLR4 axis and inhibition of tumor growth and metastasis. *Theranostics* 2024;14:2605-21.
77. Rosty C, Ueki T, Argani P, Jansen M, Yeo CJ, Cameron JL, et al. Overexpression of S100A4 in pancreatic ductal adenocarcinomas is associated with poor differentiation and DNA hypomethylation. *Am J Pathol* 2002;160:45-50.
78. Kozono S, Ohuchida K, Ohtsuka T, Cui L, Eguchi D, Fujiwara K, et al. S100A4 mRNA expression level is a predictor of radioresistance of pancreatic cancer cells. *Oncol Rep* 2013;30:1601-8.
79. Mahon PC, Baril P, Bhakta V, Chelala C, Caulee K, Harada T, Lemoine NR. S100A4 contributes to the suppression of BNIP3 expression, chemoresistance, and inhibition of apoptosis in pancreatic cancer. *Cancer Res* 2007;67:6786-95.
80. Burnett AS, Quinn PL, Ajibade DV, Peters SR, Ahlawat SK, Mahmoud OM, Chokshi RJ. Design of an immunohistochemistry biomarker panel for diagnosis of pancreatic adenocarcinoma. *Pancreatology* 2019;19:842-9.
81. Jia F, Liu M, Li X, Zhang F, Yue S, Liu J. Relationship between S100A4 protein expression and pre-operative serum CA19.9 levels in pancreatic carcinoma and its prognostic

- significance. *World J Surg Oncol* 2019;17:163.
82. Liang L, Luo R, Ding Y, Liu K, Shen L, Zeng H, et al. S100A4 overexpression in pancreatic ductal adenocarcinoma: imaging biomarkers from whole-tumor evaluation with MRI and texture analysis. *Abdom Radiol (NY)* 2021;46:623-35.
 83. Fei F, Qu J, Zhang M, Li Y, Zhang S. S100A4 in cancer progression and metastasis: A systematic review. *Oncotarget* 2017;8:73219-39.
 84. Wu Y, Zhou Q, Guo F, Chen M, Tao X, Dong D. S100 Proteins in Pancreatic Cancer: Current Knowledge and Future Perspectives. *Front Oncol* 2021;11:711180.
 85. Che P, Yang Y, Han X, Hu M, Sellers JC, Londono-Joshi AI, et al. S100A4 promotes pancreatic cancer progression through a dual signaling pathway mediated by Src and focal adhesion kinase. *Sci Rep* 2015;5:8453.
 86. Zhou Y, Li Z, Ding Y, Zhang J, Yang Q, Wu Y. Overexpression of S100A4 protein may be associated with the development and progression of pancreatic cancer. *J Cancer Res Ther* 2018;14:S159-S66.
 87. Emmanouilidi A, Paladin D, Greening DW, Falasca M. Oncogenic and Non-Malignant Pancreatic Exosome Cargo Reveal Distinct Expression of Oncogenic and Prognostic Factors Involved in Tumor Invasion and Metastasis. *Proteomics* 2019;19:e1800158.
 88. Comandatore A, Immordino B, Balsano R, Capula M, Garajova I, Ciccolini J, et al. Potential Role of Exosomes in the Chemoresistance to Gemcitabine and Nab-Paclitaxel in Pancreatic Cancer. *Diagnostics (Basel)* 2022;12.
 89. Collisson EA, Bailey P, Chang DK, Biankin AV. Molecular subtypes of pancreatic cancer. *Nat Rev Gastroenterol Hepatol* 2019;16:207-20.
 90. Porter RL, Magnus NKC, Thapar V, Morris R, Szabolcs A, Neyaz A, et al. Epithelial to mesenchymal plasticity and differential response to therapies in pancreatic ductal adenocarcinoma. *Proc Natl Acad Sci U S A* 2019;116:26835-45.
 91. Bailey P, Chang DK, Nones K, Johns AL, Patch AM, Gingras MC, et al. Genomic analyses identify molecular subtypes of pancreatic cancer. *Nature* 2016;531:47-52.
 92. Moffitt RA, Marayati R, Flate EL, Volmar KE, Loeza SG, Hoadley KA, et al. Virtual microdissection identifies distinct tumor- and stroma-specific subtypes of pancreatic ductal adenocarcinoma. *Nat Genet* 2015;47:1168-78.
 93. Collisson EA, Sadanandam A, Olson P, Gibb WJ, Truitt M, Gu S, et al. Subtypes of

- pancreatic ductal adenocarcinoma and their differing responses to therapy. *Nat Med* 2011;17:500-3.
94. Chan-Seng-Yue M, Kim JC, Wilson GW, Ng K, Figueroa EF, O'Kane GM, et al. Transcription phenotypes of pancreatic cancer are driven by genomic events during tumor evolution. *Nat Genet* 2020;52:231-40.
 95. Kim S, Leem G, Choi J, Koh Y, Lee S, Nam SH, et al. Integrative analysis of spatial and single-cell transcriptome data from human pancreatic cancer reveals an intermediate cancer cell population associated with poor prognosis. *Genome Med* 2024;16:20.
 96. Dahlmann M, Kobelt D, Walther W, Mudduluru G, Stein U. S100A4 in Cancer Metastasis: Wnt Signaling-Driven Interventions for Metastasis Restriction. *Cancers (Basel)* 2016;8.
 97. Prasmickaite L, Tenstad EM, Pettersen S, Jabeen S, Egeland EV, Nord S, et al. Basal-like breast cancer engages tumor-supportive macrophages via secreted factors induced by extracellular S100A4. *Mol Oncol* 2018;12:1540-58.
 98. Geng X, Chen H, Zhao L, Hu J, Yang W, Li G, et al. Cancer-Associated Fibroblast (CAF) Heterogeneity and Targeting Therapy of CAFs in Pancreatic Cancer. *Front Cell Dev Biol* 2021;9:655152.
 99. Zhang T, Ren Y, Yang P, Wang J, Zhou H. Cancer-associated fibroblasts in pancreatic ductal adenocarcinoma. *Cell Death & Disease* 2022;13.
 100. Yang D, Liu J, Qian H, Zhuang Q. Cancer-associated fibroblasts: from basic science to anticancer therapy. *Exp Mol Med* 2023;55:1322-32.
 101. Zeng, Pöttler, Lan, Grützmann, Pilarsky, Yang. Chemoresistance in Pancreatic Cancer. *International Journal of Molecular Sciences* 2019;20.
 102. Lin Q, Serratore A, Niu J, Shen S, Roy Chaudhuri T, Ma WW, et al. Fibroblast growth factor receptor 1 inhibition suppresses pancreatic cancer chemoresistance and chemotherapy-driven aggressiveness. *Drug Resist Updat* 2024;73:101064.
 103. Brumskill S, Barrera LN, Calcra P, Phillips C, Costello E. Inclusion of cancer-associated fibroblasts in drug screening assays to evaluate pancreatic cancer resistance to therapeutic drugs. *J Physiol Biochem* 2023;79:223-34.
 104. Schuth S, Le Blanc S, Krieger TG, Jabs J, Schenk M, Giese NA, et al. Patient-specific modeling of stroma-mediated chemoresistance of pancreatic cancer using a three-dimensional organoid-fibroblast co-culture system. *J Exp Clin Cancer Res* 2022;41:312.

105. Wittwer NL, Brown MP, Liapis V, Staudacher AH. Antibody drug conjugates: hitting the mark in pancreatic cancer? *J Exp Clin Cancer Res* 2023;42:280.
106. Xing L, Lv L, Ren J, Yu H, Zhao X, Kong X, et al. Advances in targeted therapy for pancreatic cancer. *Biomed Pharmacother* 2023;168:115717.
107. Yao H, Song W, Cao R, Ye C, Zhang L, Chen H, et al. An EGFR/HER2-targeted conjugate sensitizes gemcitabine-sensitive and resistant pancreatic cancer through different SMAD4-mediated mechanisms. *Nat Commun* 2022;13:5506.
108. Zheng C, Zhou D, Li W, Duan Y, Xu M, Liu J, et al. Therapeutic efficacy of a MMAE-based anti-DR5 drug conjugate Oba01 in preclinical models of pancreatic cancer. *Cell Death Dis* 2023;14:295.
109. Nishigaki T, Takahashi T, Serada S, Fujimoto M, Ohkawara T, Hara H, et al. Anti-glypican-1 antibody-drug conjugate is a potential therapy against pancreatic cancer. *Br J Cancer* 2020;122:1333-41.
110. Zhou L, Wang Q, Zhang H, Li Y, Xie S, Xu M. YAP Inhibition by Nuciferine via AMPK-Mediated Downregulation of HMGCR Sensitizes Pancreatic Cancer Cells to Gemcitabine. *Biomolecules* 2019;9.

Abstract in Korean

췌장암 세포주에서 3D 오가노이드 배양 방법을 이용한
Gemcitabine과 Abraxane (nab-paclitaxel) 조합 항암제
감수성 효과 예측 마커 유전자 발굴

췌장암은 5년 생존율이 10% 미만으로 여전히 치명적인 악성질환으로 남아있다. 전체 췌장암 환자의 80% 이상이 수술적 절제가 불가능한 단계에서 진단되고 있어 이들의 경우 항암치료가 필요하다. 하지만 아직 환자 맞춤형 약물 선택을 위한 바이오마커가 없기 때문에 췌장암 환자를 위한 바이오마커의 발굴은 필수적이다.

이를 위한 첫 번째 시도 중 하나는 환자의 종양으로부터 부착형 췌장암 세포주 (2D)를 확립한 것이다. 수십 년 동안 이러한 2D 췌장암 세포주는 편리한 PDAC 모델로 사용되어 왔다. 그러나 2D 세포는 종양의 미세환경, 물질대사, 항암제에 대한 민감성, 유전자발현 등 여러 측면에서 초기 종양의 특징과 다소 차이가 있다. 이러한 차이를 줄이기 위한 방법으로 최근 췌장, 전립선, 간, 위, 폐 등 장기에 영향을 미치는 다양한 암 유형에 대해 3D 종양 오가노이드 배양 방법이 개발되었다. 오가노이드는 원종양의 형태, 유전자 및 단백질 발현, 세포 극성 및 세포 대사 이질성을 크게 재현할 수 있다. 결과적으로 췌장암의 모델링 및 약물 테스트를 수행하는 데 이상적인 도구 역할을 한다.

본 연구에서는 겐시타빈과 아브락산(nab-paclitaxel) 조합 항암제의 효능에 대한 예측 마커 유전자를 확인하고 췌장암의 치료 효과를 높이기 위하여 오가노이드 배양 배지를 사용하지 않고 일반 배양 배지 조건에서 췌장암 세포주와 F-배지 조건에서 환자 유래 췌장암 세포주 (CRC YPAC 세포주)를 활용하여 매트릭스 기반의 3D 오가노이드 배양 모델 및 오가노이드 약물 테스트 플랫폼을 구축하였다. 나아가 수립한 오가노이드 배양 모델 및 약물 테스트 플랫폼을 활용하여 췌장암에서 겐시타빈과 아브락산(nab-paclitaxel) 조합 항암제에 대한 민감성 바이오마커로 IL4R을, 저항성 바이오마커로 S100A4를 확인하였다.

핵심되는 말: 췌장암 세포주, 첼시타빈과 아브락산 (nab-paclitaxel) 조합 항암제, 3D 오가노이드 배양 모델, 예측 마커 유전자